ROOM-TEMPERATURE PHOSPHATE CERAMICS MADE WITH AFŞİN-ELBİSTAN FLY ASH

A THESIS SUBMITTED TO
THE GRADUATE SCHOOL OF NATURAL AND APPLIED SCIENCES
OF
MIDDLE EAST TECHNICAL UNIVERSITY

BY
MAHDI MAHYAR

IN PARTIAL FULFILLMENT OF THE REQUIREMENTS
FOR
THE DEGREE OF MASTER OF SCIENCE
IN
CIVIL ENGINEERING

SEPTEMBER 2014

Approval of the thesis:

ROOM-TEMPERATURE PHOSPHATE CERAMICS MADE WITH AFŞİN-ELBİSTAN FLY ASH

submitted by **MAHDI MAHYAR** in partial fulfillment of the requirements for the degree of **Master of Science in Civil Engineering Department**, **Middle East Technical University** by,

Prof. Dr. Canan Özgen _____
Dean, Graduate School of **Natural and Applied Sciences**

Prof. Dr. Ahmet Cevdet Yalçıner _____
Head of Department, **Civil Engineering**

Assoc. Prof. Dr. Sinan Turhan Erdoğan
Supervisor, **Civil Engineering Dept., METU** _____

Examining Committee Members:

Prof. Dr. Mustafa Tokyay _____
Civil Engineering Dept., METU

Assoc. Prof. Dr. Sinan Turhan Erdoğan _____
Civil Engineering Dept., METU

Assoc. Prof. Dr. Lutfullah Turanlı _____
Civil Engineering Dept., METU

Assoc. Prof. Dr. Caner Durucan _____
Metallurgical and Materials Engineering Dept., METU

Assist. Prof. Dr. Çağla Meral _____
Civil Engineering Dept., METU

Date: 03.09.2014

I hereby declare that all information in this document has been obtained and presented in accordance with academic rules and ethical conduct. I also declare that, as required by these rules and conduct, I have fully cited and referenced all material and results that are not original to this work.

Name, Last name: Mahdi Mahyar

Signature :

ABSTRACT

ROOM-TEMPERATURE PHOSPHATE CERAMICS MADE WITH AFŞİN-ELBİSTAN FLY ASH

Mahyar, Mahdi
M.Sc., Department of Civil Engineering
Supervisor: Assoc. Prof. Dr. Sinan Turhan Erdoğan

September 2014, 85 pages

The mechanical behavior and microstructure of acid-base phosphate ceramics produced at room temperature using coal fly ash from Afşin Elbistan (AE) thermal power plant were investigated. The main goal was to introduce a novel application for this industrial waste which does not meet the standards for use in the cement and concrete industry.

Chemically-bonded phosphate ceramics (CBPC) can provide certain advantages over ordinary Portland cement products such as better mechanical strength, better durability, shorter setting time, better high temperature resistance and a lower carbon footprint. The chemical composition of AE fly ash indicated its potential for CBPC production.

Activation of the fly ash was done using two phosphate sources; a phosphoric acid solution or a phosphoric acid salt (monopotassium dihydrogen phosphate). Various phosphoric acid solution concentrations and different solution-to-powder ratios

were used. To achieve comparable results, acid salt contents with phosphate ion contents equivalent to those of the solutions were chosen. Partial replacement of the fly ash with soda lime glass and calcium aluminate cement was also studied. Compressive strengths were measured up to age 28 days. The microstructure and morphology of reaction products were investigated using scanning electron microscopy. X-ray fluorescence spectrometry was used to determine the chemical analyses of raw materials and x-ray diffraction was used to investigate the crystalline reaction products.

Pastes incorporating a 60 wt% solution of phosphoric acid and a solution-to-powder ratio one of 1.0 exhibited the highest performance. AE fly ash pastes, loaded with 10 wt% soda lime glass, and activated with 60 wt% phosphoric acid solution and a solution-to-powder ratio of 1.0 reached the highest 28-day compressive strength with 30 MPa.

Keywords: Fly ash, Chemically bonded phosphate ceramic

ÖZ

ODA SICAKLIĞINDA AFŞİN ELBİSTAN UÇUCU KÜLÜNDEN ÜRETİLEN FOSFAT SERAMİKLER

Mahyar, Mahdi
Yüksek Lisans, İnşaat Mühendisliği Bölümü
Tez Yöneticisi: Doç. Dr. Sinan Turhan Erdoğan

Eylül 2014, 85 sayfa

Afşin Elbistan (AE) termik santralinden elde edilen kömür uçucu külü ile oda sıcaklığında üretilen asit-baz fosfat seramiklerinin mekanik ve mikroyapıları incelenmiştir. Ana hedef çimento ve beton sanayiinde kullanım için gerekli standartlara uymayan bu endüstriyel atık için yeni bir uygulama sunmaktır.

Kimyasal olarak bağlanmış fosfat seramikler, (KBFS) Portland çimentolu ürünlere kıyasla üstün mekanik özelikler, daha yüksek dayanıklılık, daha kısa priz süresi, daha olumlu yüksek sıcaklık dayanıklılığı, ve daha düşük karbon ayakizi sunabilmektedir. AE uçucu külünün kimyasal kompozisyonu KBFS üretiminde kullanılabileceğine işaret etmektedir.

Uçucu külün aktivasyonu iki fosfat kaynağı, fosforik asit çözeltisi veya bir fosforik asit tuzu (monopotasyum dihidrojen fosfat) kullanılarak gerçekleştirilmiştir. Farklı fosforik asit çözelti konsantrasyonları ve farklı çözelti-toz oranları kullanılmıştır. Karşılaştırılabilir sonuçlar elde etmek için çözeltilerdeki fosfat iyonuna denk

miktarda iyon barındıracak miktarda asit tuzu seçilmiştir. Uçucu külün soda kireç camı ve kalsiyum alüminatlı çimento ile kısmen yer değiştirilmesi de çalışılmıştır. Basınç dayanımı 28. güne kadar ölçülmüştür. Tepkime ürünlerinin morfolojisi ve mikroyapısı taramalı elektron mikroskopisi (TEM) kullanılarak incelenmiştir. Ham maddelerin kimyasal kompozisyonu X-ışını floresans spektrometresi (XIF) kullanılarak, kristal yapılı tepkime ürünleri x-ışını kırılması (XIK) kullanılarak belirlenmiştir.

Kütlece % 60 fosforik asit çözeltisi ve 1,0 çözelti-toz oranı ile yapılan hamurlar en iyi performansı vermiştir. % 10 soda kireç camı içeren ve kütlece % 60 fosforik asit çözeltisi ile 1,0 çözelti-toz oranıyla hazırlanan AE uçucu külü hamurları 30 MPa 28. gün basınç dayanımına ulaşmıştır.

Anahtar Kelimeler: Uçucu Kül, Fosfat Seramik

To my wife

Nasim

ACKNOWLEDGMENTS

I wish to express my gratitude towards my advisor, Dr. Sinan Turhan Erdoğan from METU for supervising my work. Thanks to his sincere care, trust and guidance, understanding, motivation and support from the beginning of my master program and during the time I worked on this thesis. I am also grateful for the financial support that he has provided me through research assistantships at METU materials of construction laboratory.

I am most grateful for the insightful recommendations of my committee members, Dr. Mustafa Tokyay, Dr. Lutfullah Turanlı, Dr. Caner Durucan and Dr. Çağla Meral whose helped to improve the quality of this thesis.

I wish to thank Dr. İsmail Özgür Yaman, for his valuable comments and contributions throughout all my education at METU.

I also want to extend my appreciation to Dr. Turhan Y. Erdoğan, for his cheerful motivation. He inspired me to work intensively and to optimize my experience at METU.

I am eternally indebted to all the members of the Materials of Construction Laboratory group, of which I am honored to be a part. Thanks to Mr. Cuma Yıldırım for his help working with equipment; Burhan, for his friendship and support; Meltem, for her friendship and sharing her raw materials; Murat and Hasan for being part of one of the best times of my life and Alireza for being a great friend, from the first day of program to the last.

And finally, I am very grateful to my wife, Nasim, for her patience, support, endurance, and her moral support encouraged me to adhere to this study.

If I neglected to mention you above, I would like to thank you very much.

TABLE OF CONTENTS

LIST OF TABLES

TABLES

LIST OF FIGURES

FIGURES

CHAPTER 1

INTRODUCTION

1.1 Background

In the past few decades, significant ecological alterations such as climate change and global warming, caused public anxiety and at higher levels, commenced debate in all fields of science and engineering. The rapid rate of growth of construction has brought out the concrete industry to be considered as one of the largest contributors to these ecological changes. U.S. Geological Survey (2013) reported that in 2012, the concrete industry produces approximately 3.7 billion tons of Portland cement worldwide. In addition to consuming considerable amounts of energy and natural materials such as limestone and sand, producing each ton of Portland cement approximately emits one ton of carbon dioxide gas (CO_2) into the environment (Mehta, 1999).

To reduce the excessive emission of CO_2 by the concrete industry, technologies emerged to approach the goal of sustainable development by using "green" materials for construction.

> Green materials are considered as materials that use less natural resource and energy and generate less CO_2. They are durable and recyclable and require less maintenance (Edvardsen and Tollose, 2001).

To compensate for utilizing virgin materials in Portland cement production or decreasing the usage rate of this hydraulic binder in concrete, industrial by-products, such as fly ash or ground granulated blast furnace slag have application in both Portland cement fabrication procedure and partial replacement of Portland cement in concrete production. Utilization of suitable industrial by-products not only saves

our planet from hazardous contamination, but also has a great impact at produced concrete performance and its durability.

Fly ash, is a residue of coal burned to provide thermal energy in power plants. The coal extracted from different sources contains various kinds of impurities inside, although ignition temperature and conditions change depending on the required field of application, hence this cause a dissimilarity in kind and proportion of composition within produced fly ash. There are criteria, according these proportions of compositions, which classify fly ash in different group. If a fly ash meets the criteria, it find an application in concrete production procedure, otherwise it is stockpiled to be left in nature.

Afşin-Elbistan fly ash (AE fly ash) is an example of a useless by-product which does not meet the needs to be utilized in concrete production, therefore this study has been conducted to investigate production of phosphate base binders using AE fly ash.

1.2 Objectives

The main objectives of this study were:

a) To investigate the possibility of producing chemically bonded phosphate ceramics/cements (CBPC) with AE fly ash
b) To search for the optimum combination of the raw materials and mixture composition
c) To determine the compressive strength of the produced CBPCs
d) To inspect the factors affecting the acid base reaction such as solubility, pH and contributing anion and cation sources and amounts
e) To compare the microstructures of the produced CBPCs via SEM, XRF, XRD techniques.

CHAPTER 2

LITERATURE REVIEW

2.1 Green Cement

From ancient times, materials taken from nature, such as wood or stone were fashioned into tools and weapons by humans. Using mud to shape a shelter can be explain as an initial binder application of mankind. Discovery of pottery, eliminated slow and time-consuming process of carving or grinding of natural material where a soft plastic body, potter's clay, is molded into the desired shape before being converted into a rigid substance by firing (Wilson and Nicholson, 2005). The Romans were pioneers in the wide-scale use of hydraulic binders. The Roman architect, Vitruvius, in an ancient treatise, reported that the Romans found a natural powder called Pozzolana which was giving astonishing results when mixed with lime and rubble. It could set hard even under water (Morgan and Warren, 1960). At the beginning of the eighteenth century Portland cement was developed from natural cements in Britain (Gillberg et al., 1999). After the introduction of Portland cement to the world, different species of this product emerged, such as, Portland blast furnace cement, Portland fly ash cement, Portland pozzolan cement, Portland silica fume cement, white cements etc. Growing environmental concerns and increasing cost of fossil fuels have resulted in production of third generation binders called "Green Cement". Green cement is a binder that meets or exceeds the functional performance capabilities of ordinary Portland cement by incorporating and optimizing recycled materials, thereby reducing consumption of natural raw materials, water, and energy, resulting in a more sustainable construction material. Greenhouse gas reduction or even elimination in the manufacturing process for green cement can be expressed as its most important goal (Gillberg et al., 1999).

2.1.1 Importance

In recent years, the concrete industry, in order to meet housing and infrastructural needs of society in a sustainable manner, has been confronted with three important issues: Climate change, Resource productivity and Industrial ecology (Mehta, 2004).

Most scientists believe that the high emission rates of greenhouse gases, primarily carbon dioxide, is the main reason of extreme weather patterns occurring with greater frequency today. The Portland cement industry is responsible for approximately 5% of the world's man-made carbon dioxide emissions (World Business Council for Sustainable Development, 2009). In addition the concrete industry is the largest consumer of virgin materials such as sand, gravel, crushed rock, and fresh water. Cement production consumes vast amounts of limestone and clay besides being energy-intensive (Mehta, 2004). By enhancing the performance of products and making them more durable, dramatic improvement can be achieved in service life and resources will be saved as well. Utilization of recycled materials and by-products not only eliminate the waste hazards to our environment but also could substitute for virgin materials in order to save remaining resources for next generations.

2.2 Fly ash

2.2.1 Introduction

Coal is an abundant fossil fuel which is used as the major energy source of electricity production plants around the world because of its availability and hence its low cost. Fly ash is an industrial by-product of coal combustion. When coal is burned, fine particles from combustion residues rise with flue gases. These fine particles are captured by various filtration methods from the flue gas in the chimney (Ahmaruzzaman, 2010). The primary components of this waste material are silica (SiO_2), iron oxides (Fe_2O_3) and alumina (Al_2O_3) , with varying amounts of carbon, calcium (as lime or gypsum), magnesium and sulfur (sulfides or sulfates) (Iyer & Scott, 2001).

2.2.2 Classification

2.2.2.1 Physical properties

Fly ash consists of fine, powdery porous particles, predominantly spherical or even asymmetrical in shape, either solid or hollow, and mostly glassy (amorphous) in nature. The particle size distribution of fly ash might differ depending on carbon content of the unburnt coal. If a coal contains 45 % to 86 % carbon, it is called bituminous coal. The particle size distribution of most bituminous coal fly ash is generally similar to that of silt (smaller than 0.075 mm or passing the No. 200 sieve). If the carbon content of coal were 35 % to 45 %, it is classified as sub-bituminous coal. Generally sub-bituminous coal fly ash is slightly coarser than bituminous coal fly ash. The specific gravity of fly ash usually ranges from 2.1 to 3.0, while its specific surface area may vary from 170 to 1000 m^2/kg (Ahmaruzzaman, 2010). The color of fly ash can vary from tan to gray to reddish brown, depending on the amount of unburnt carbon in the ash (Roy et al., 1981).

2.2.2.2 Chemical properties

In general since burnt coal in power plants or other furnaces are not identically similar in their chemical compositions, and since differences exist in combustion temperature and conditions, the composition of captured fly ashes differ slightly. According to ASTM standard, there are mainly two types of fly ash produced from coal combustion, types F and C. Type F is produced when anthracite (coal with 86 % to 97 % carbon content), bituminous or sub-bituminous coal is burned and it is low in lime (< 7 %) and high in silica, alumina and iron oxide. Type C comes from lignite coal combustion (coal with 25 % to 35 % carbon content) and contains higher lime (15-30 %) (Fisher and Prentice, 1978).

2.2.3 Disposal

The most widely accepted disposal methods for fly ash are stockpiling and landfilling. Dispersion of bare fly ash near the landfill, because of wind is inevitable. High costs of stabilization to achieve a safe disposal, decrease of world-wide available areas for landfilling, can be the main concerns of fly ash disposal. Seaport filling and deep water disposal have been used as fly ash disposal methods as well. Because of the typical chemical compositions of fly ash, it can be considered a toxic

waste hence this disposal methods will eventuate to several environmental problems (Ferraiolo et al., 1990).

2.2.4 Environmental Impact

The environmental impacts of fly ash in terms of its massive generation, usage of land for disposal, short and long term impacts on surrounding areas are well known. The principal environmental concern stems from the possible leaching of metals and organic compounds and their migration into ground water or nearby surface water. In addition, fly ash could also affect human health through direct inhalation or ingestion of airborne or settled ash (Kumar et al., 2007).

2.2.5 General Utilization

Before dedicating a waste material for an application area, three major factors must be taken into account. The first factor is “suitability for processing”. Depending on the physical and chemical properties of fly ash there are limitations for specific processes. “Technical performance” is the second factor. Even if fly ash can be easily processed, the final product cannot be used unless it presents good technical properties. The third and last factor is “environmental impact”. Toxicity does not necessarily disappear with fly ash re-utilization. The risks imposed on the environment by each possible application must be carefully analyzed against creating new pollution sources elsewhere. Potential applications for fly ash are grouped into followings: construction materials (cement production, concrete, ceramics, glass and glass–ceramics), geotechnical applications (road pavement and embankments), agriculture and miscellaneous (sorbent and sludge conditioning) (Ferreira et al., 2003).

2.2.6 Applications in construction

Fly ash has vast applications in cement and concrete manufacture. It can be used replace of cement in Portland cement concrete at ready mix plants or as a pozzolanic material in the production of pozzolanic cements in cement factories, and even as a set retardant with cement as a replacement of gypsum (Ahmaruzzaman, 2010).

ASTM C595 (2012) defines two blended cement products in which fly ash has been added:

1. Portland-pozzolan cement (Type IP), containing 15 % to 40 % pozzolan
2. Pozzolan modified Portland cement (Type I-PM), containing less than 15 % pozzolan

ASTM C618 (2012) delineates requirements for the physical, chemical, and mechanical properties for these two classes of fly ash. Class F fly ash is pozzolanic, with little or no cementing value alone. Class C fly ash has self-cementing properties as well as pozzolanic properties.

Table 2.1 Chemical requirements for fly ash classification (ASTM C618).

	Class	
	F	C
Silicon dioxide (SiO_2) plus aluminum oxide (Al_2O_3) plus iron oxide (Fe_2O_3), min, %	70.0	50.0
Sulfur trioxide (SO_3), max, %	5.0	5.0
Moisture content, max, %	3.0	3.0
Loss on ignition, max, %	6.0	6.0

2.2.7 Afşin Elbistan Fly Ash

Afşin Elbistan (AE) thermal power plants (parts A and B) are located at Kahramanmaraş province in Turkey. These power plant are fed with a local coal deposit with same name. Generally, physical properties and chemical composition of a fly ash depend on the mineral composition of the burnt coal. In Afşin Elbistan

deposit, the coal seam consists of clay, marl and sandy clay. The existence of these impurities within the extracted coal, affect the properties of AE fly ash (Ural, 2005).

Coal production is exploited in Kışlakoy opencast mine which supplies feed coal to AE power plant part A, which has four boiler units each with 340 MW capacity. Only AE power plant part A, consumes approximately 18.0×10^6 metric tons of coal per year and generates about 3.24×10^6 metric tons of fly ashes. These ashes are returned to the dumping area of the mine as combustion waste (Ural, 2005).

Based on a study done on four successive days, the CaO contents of the fly ash samples, derived from both AE power plant part A and B, were higher than 10 %. According to ASTM C618 (Table 2.1), if the sum of SiO_2, Al_2O_3 and Fe_2O_3 is higher than 50 % of total compositions and CaO amount is higher than 10 %, fly ash, classified as class C. Despite of the high CaO contents, the total amounts of $SiO_2+Al_2O_3+Fe_2O_3$ in AE fly ash for both units is less than 50 % and also the total content of sulfur (SO_3) which must be less than 5 % in accordance with ASTM C618 (2012), measured as 11.41 % for AE power plant part B and 24.24 % for part A (Türker et al., 2009). Hence AE fly ash doesn't meet the requirements of ASTM C618 (2012) for class C fly ash and it is not allowed to be utilized in Portland blended cement or partial cement substitution in concrete production.

2.3 Ceramics

2.3.1 Conventional Ceramics vs. Hydraulic Cements

Traditionally man-made inorganic solids were divided into two major classes of ceramics and hydraulic cements. Hydraulic cements harden at room temperature when their powder is mixed with water. The formed paste sets into a hard mass which has sufficient compressive strength to be used as a structural material. Their structures are generally non-crystalline. Hydraulic cements are an example of accelerated chemical bonding. Hydrogen bonds are formed inside these materials by chemical reaction when water is added to the powders. Portland cement, calcium aluminate cement, and plaster of Paris are typical examples of this group (Wilson and Nicholson, 2005). On the other hand, ceramics are formed by compaction of powders and then fusion at high temperatures, ranging from 700 to 2000˚C. Once

fused, the produced ceramics are hard, dense, and have very good durability. They are generally highly crystalline with some glassy phases as well.

During production, ceramics are exposed to intense heat treatment for their consolidation whilst cement products are formed by chemical reaction at room temperature. However, their differences go beyond this. From a structural viewpoint, the distinction between ceramics and cements is related with the interparticle bonds that holds them together and provides strength. Hydraulic cements are bonded by hydrogen bonding and van der Waals forces, while ceramics are formed by either ionic or covalent bonds between their particles. Since covalent and ionic bonds are stronger than van der Waals bonds, ceramics are stronger than cements. Ceramics are also less porous than hydraulic cements and they can tolerate very high temperatures, and are durable in a wide range of pH, whilst most of hydraulic cements are affected by high temperature as well as acidic environment (Wagh, 2004). There are also exceptions for hydraulic cements such as calcium aluminate cement which can undergo high temperatures. In addition a disadvantage of ceramics can be their high cost. Since they are sintered at very high temperatures, they are costliest than cements.

2.3.2 Chemically-bonded ceramics

Chemically bonded ceramics (CBCs) rely on low temperature solid-liquid reactions to effect the formation of new phases which serve as a glue holding ceramic particles together (Roy et al., 1991). At first glance, they appear similar to hydraulic cements. While a powder and a liquid react chemically and give strength to the final product at room temperature. The main distinction is in their bonding mechanism. Similar to ceramics, they have covalent and ionic bonding in their structure (Wagh, 2004) and they are highly crystalline. The name chemically bonded ceramics (CBCs) was coined by Roy (1987). Wilson and Nicholson (2005) have classified this type of binders as “condensation cements”.

CBCs have been widely used for multiple applications combining structural properties of ceramics with the easy fabrication of conventional cements. Utilization of these binders as replacements for conventional cement could significantly reduce

the overall consumption of energy and greatly restrict the environmental impacts of processing, production, and disposal (Laufenberg et al., 2004).

2.4 Acid-base cements

Acid-base (AB) cements have been known since the mid-19th century. They are formed by the interaction of an acid and a base, a reaction which yields a cementitious salt hydrogel (Wilson, 1978). A proton donating liquid (H_2A) and a powder which acts as a proton acceptor (MO) react to produce salt gel (MA) and water. The generic setting reaction may be simply represented as:

$$MO + H_2A \rightarrow MA + H_2O \qquad (2.1)$$

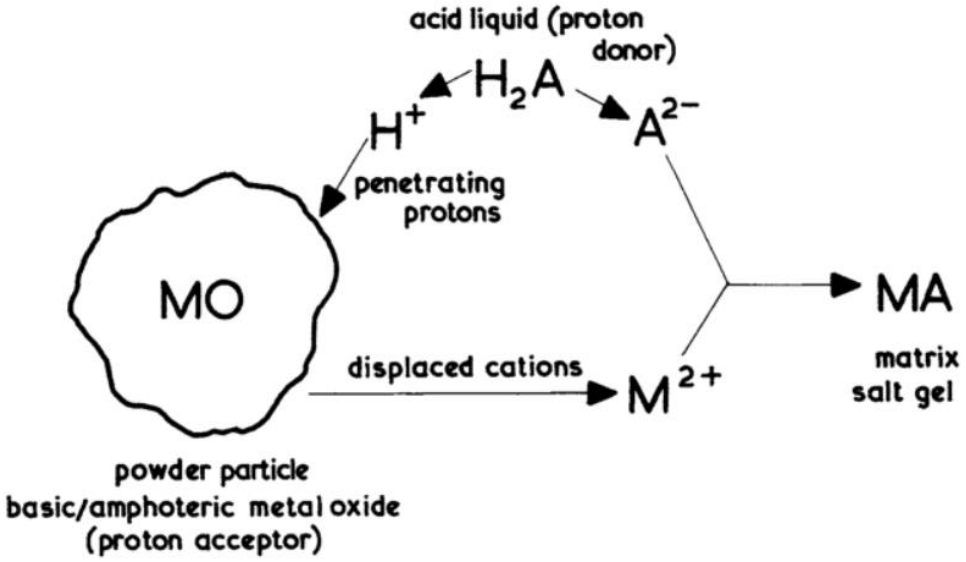

Figure 2.1. Schematic representation of setting reaction in acid-base cement (Wilson et al., 1979).

For convenience of representation in Figure 2.1, the oxide cation and the liquid anion are taken as being divalent. In fact, H_2A may represent phosphoric acid and M can represent Al as well as Zn, Mg, Ca or other metals (Wilson et al., 1979).

Normally the reaction between an acid and a base produces a noncoherent precipitate. If, however, the reaction rate is controlled properly between certain acids and bases, coherent bonds can develop between precipitating particles that will grow into crystalline structures and form a ceramic. The acidic and alkaline components neutralize each other rapidly, and the resulting paste sets rapidly into products with neutral pH (Wagh, 2004). However formation of acid-base cements involves both acid-base and hydration reactions and after initial setting by acid base reaction, hydration continues to strengthen the final product with time (Wilson et al., 1979). Desired compressive strength and very rapid setting characteristic of these materials have allowed them to find diverse applications, ranging from biomedical to industrial (Wilson and Nicholson, 2005). Wagh (2004) divided acid-base cements into three main categories: Polyalkenoate Cements, Oxysalt Cements and Chemically Bonded Phosphate Ceramics.

2.4.1 Polyalkenoate cements

The polyalkenoate cements are modern materials that have adhesive properties and are formed by the cement-forming reaction between a poly (alkenoic acid), typically poly acrylic acid in concentrated aqueous solution, and a cation-releasing base. The base may be a metal oxide, in particular zinc oxide, a silicate mineral or an aluminosilicate glass. The presence of a poly acid in these cements gives them the valuable property of adhesion (Wilson and Nicholson, 2005).

2.4.2 Oxysalts cements

Oxysalt bonded cements are formed by acid-base reactions between a metal oxide in powdered solid form and aqueous solutions of metal chloride or sulphate. The three major types of oxysalt bonded AB cement are the zinc oxychloride, the magnesium chloride and the magnesium oxysulphate cements (Wilson and Nicholson, 2005).

2.4.3 Chemically-bonded phosphate ceramics

Chemically bonded phosphate ceramics (CBPCs) belong to the CBC and acid-base families and are formed by reacting a source of a metal cation, such as a metal oxide, with a source of a phosphate anion, such as phosphoric acid or an acid phosphate (Wagh and Jeong, 2003). The oldest use of CBPC is in the preparation of dental cements. The main type is a mixture of zinc oxide and phosphoric acid for forming a cement for fillings, caps, etc. Another type of dental cement called "porcelain" consisted of powdered alumina-lime-silica glass mixed with phosphoric acid to form a hard white translucent product (Kingery, 1948). CBPC products are now finding applications in diverse fields that include structural ceramics, waste management, oil drilling and completions, and bioceramics. The inorganic and nontoxic nature of products made with CBPCs and their neutrality and stability in a wide range of pH could be their most important advantages (Wagh, 2004).

2.4.3.1 Kinetics of Formation of CBPCs

Water has a vital role in the formation of CBCs. It act as a medium to solve materials to enable them for reaction. First, dissolution of the acid leads to the formation of phosphate ions and protons in the solution and makes the solution acidic. A phosphoric acid molecule can dissociate up to three times, giving up an H^+ each time, which typically combines with a water molecule, H_2O, as shown in these reactions:

$$H_3PO_4 + H_2O \rightarrow H_3O^+ + H_2PO_4^- \quad (2.2)$$

$$H_2PO_4^- + H_2O \rightarrow H_3O^+ + HPO_4^{2-} \quad (2.3)$$

$$HPO_4^{2-} + H_2O \rightarrow H_3O^+ + PO_4^{3-} \quad (2.4)$$

The anion after the first dissociation, $H_2PO_4^-$, is the dihydrogen phosphate anion. The anion after the second dissociation, HPO_4^{2-}, is the hydrogen phosphate anion. The anion after the third dissociation, PO_4^{3-}, is the phosphate anion.

Wagh (2004) classified the formation of CBPCs into three main steps:

Step 1. Aquosol formation by dissolution: When metal oxides are stirred into an acid solution, they start to dissolve in the solution, releasing their own metal that contains cations and oxygen-containing anions (Figure 2.2a). The cations react with water molecules and form positively charged "aquosols" by hydrolysis (Figure 2.2b).

Step 2. Acid–base reaction and the formation of gel by condensation: The sols subsequently react with the aqueous phosphate anions to form the hydrophosphate salts, while the protons and oxygen react to form water. As the oxide powder is stirred in water, more aquosols are formed in the solution and they start connecting to each other (Figure 2.2c). This leads to the formation of a gel of loosely connected salt molecules (Figure 2.2d).

Step 3. Saturation and crystallization of the gel into a ceramic: As the reaction proceeds, this process introduces more and more reaction products into the gel, and it thickens. At this point, it becomes difficult to mix the slurry. The gel now crystallizes around the unreacted core of each grain of the metal oxide into a well-connected crystal lattice that grows into a monolithic ceramic (Figure 2.2e).

The dissociation speed of cations from the metal oxide in the acid solution determines whether the final reaction product becomes a well-crystallized ceramic or a poorly crystalline precipitate.

In general the dissolution speed should be high enough for the formation of a saturated gel, and low enough to allow slow crystallization of the gel. The produced heat also should be controlled by oxide dissolution to be low enough to allow a well-ordered crystalline ceramic structure otherwise it will interrupt crystallization (Wagh, 2004). In other words, both the rate at which the structure is formed and the rate at which the metal ions are released must be balanced. If the rate of release of cations is too fast a non-coherent precipitate will be produced and the gel formed slowly, the crystal structure will be interrupted (Natarajan, 2005).

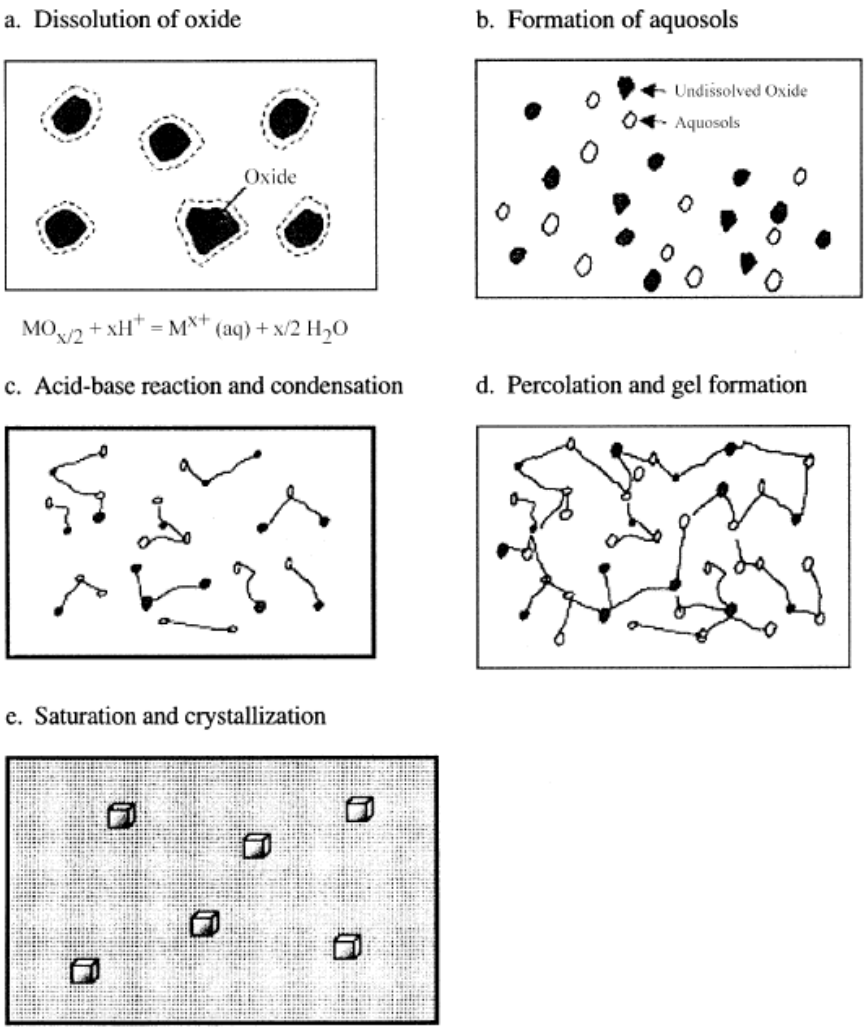

Figure 2.2 Schematic representation of the formation of chemically-bonded phosphate ceramic (Wagh, 2004).

2.4.3.2 Solubility of metal oxides

The "solubility product constant" which is the equilibrium constant of the corresponding solubility reaction defines the solubility rate of a metal oxide in an acid environment. A general solubility equation can be:

$$MX_{(s)} \rightarrow M^{+}_{(aq)} + X^{-}_{(aq)} \quad (2.5)$$

where, MX is a metal oxide, M^+ and X^- are the cation and anion, respectively. "s" and "aq" stand for "solid" and "aqueous", respectively. Therefore the solubility product constant (K_{sp}) can be written as:

$$K_{sp} = \frac{[M^+][X^-]}{[MX]} \quad (2.6)$$

$$K_{sp} = \left[M_{aq}{}^{+}\right][X^-] \quad (2.7)$$

K_{sp} is a quantitative measure of the amount of dissolution of a product in an solution, and in the case of the acid solution, it depends on the pH the of solution(Wagh and Jeong, 2003). Solubility of the metal cations depend on the acidity of the acid solution and solubility decreases as the pH of the system increases. The acid phosphate solution pH changes depending on the concentration of the acid (Natarajan, 2005). By considering a phosphoric acid (H_3PO_4) with pH < 2.1, there is no dissolution of the acid, the region of 7.2 > pH > 2.1 is suitable for reaction in which the major dissolution products are $H_2PO_4^-$ and HPO_4^{2-} . The major part of reaction occurs at pH > 2.1 and the minor portion occurs at pH ~ 7.2 (Wagh and Jeong, 2003).

As mentioned earlier, oxides should exhibit low enough solubility if they are to form useful ceramics. Wagh (2004) reported that:

> The solubility should not be too high to form a precipitate or too low to react insufficiently. Monovalent metal oxides with the exception of Ag_2O and Cu_2O are soluble in water; divalent oxides are generally sparsely soluble; trivalent oxides are even less soluble (with few exceptions such as yttria and bismuth oxide); and oxides of higher

valency are mostly insoluble. Therefore, monovalent oxides dissolve rapidly in the phosphate solution and form phosphate precipitates without forming monolithic ceramics. Sparsely soluble divalent oxides are most suitable for the formation of well-crystallized ceramics. Tri- and quadrivalent oxides do not dissolve sufficiently; hence, it has been difficult to form ceramics by their dissolution.

2.4.3.3 Metal oxide candidates for CBPC production

The solubility of metal oxides in acid phosphate solutions and their availability are the two main factors in their selection for CBPC fabrication. Kingery (1950) divided metal oxides into two groups, oxides of weak basic metals such as aluminum, zinc, beryllium and magnesium which have produced good cements and oxides of more basic metals, for example calcium, barium and thorium, which weaken the cement. He also subdivided the oxide reaction with phosphoric acid into three groups. The first group, comprises no reaction with an acidic or inert nature oxides such as SiO_2, Al_2O_3, ZrO_2 and Co_2O_3. Second group, describes a violent reaction with reactive oxides such as CaO, SrO, BaO and La_2O_3, yielding non-cementitious products, which are crystalline, porous and friable. Their reactions can be affected by calcining the oxide such as calcined CaO, which can form cements when phosphoric acid is partly neutralized by CaO. The third and last group defines a controlled reaction with cement formation. BeO, $Be(OH)_2$, CuO, Cu_2O, CdO, SnO and Pb_3O_4 as well as calcined ZnO and MgO can form cements (Wilson and Nicholson, 2005).

Wagh (2004) compared the solubility of metal oxides by pH and used the Equation (2.8) to explain the relation between the available metal cations for the reaction and the pH of the acid phosphate solution.

$$\log[M^{n+}{}_{(aq)}] = pK_{sp} - n\text{pH} \quad (2.8)$$

where:

pK_{sp} = -log K_{sp}

pH = -log [H^-]

n = The valency of the metal oxide

In Equation 2.8, if $pK_{sp} - n$pH is bigger than zero, then the concentration of the dissolved cations in the solution given by log[$M^{n+}{}_{(aq)}$] will be large, indicating a rapid dissolution of the species. For slow dissolution to occur $pK_{sp} - n$pH should be negative. In other words *n*pH must be greater than pK_{sp}. The minimum pH to allow this, is $pH_{min} = pK_{sp}/n$ and the value of this pH_{min} should fall in the near neutral region for the formation of cement by acid base reaction (Wagh, 2004). From Table 2.1, it is seen that pH_{min} of ZnO, FeO, and MgO falls in the near neutral region. Therefore it should be possible to form CBCs using these oxides. The CaO has a pH_{min} value of 11.48, which is very high and hence it is not possible to form CBCs with CaO. On the opposite side pH_{min} for Al_2O_3 and Fe_2O_3 is too low, Therefore again these two oxides may not suitable for CBC (Natarajan, 2005).

Table 2.2 pKsp values of some of metal oxides (Wagh, 2004).

Metal Oxide	Reaction	pK_{sp}	pH_{min}
ZnO	$ZnO + 2H^+ = Zn^{2+}(aq) + H_2O$	10.96	5.48
CaO	$CaO + 2H^+ = Ca^{2+}(aq) + H_2O$	22.91	11.46
FeO	$FeO + 2H^+ = Fe^{2+}(aq) + H_2O$	13.29	6.65
MgO	$MgO + 2H^+ = Mg^{2+}(aq) + H_2O$	16.95	8.48
Al_2O_3	$AlO_{3/2} + 3H^+ = Al^{3+}(aq) + H_2O$	8.55	2.85
	$AlO_{3/2} + 1/2H^+ = Al^{2-}(aq) + H_2O$	11.76	3.92
Fe_2O_3	$Fe_2O_3 + 6H^+ = 2Fe^{3+} + 3H_2O$	-0.72	-0.24

2.4.3.4 Reaction retardment and setting time control

According to a US patent (Wagh and Jeong, 2002):

> As for the retardant, boric acid, borax, sodium tripolyphosphate, sodium sulfonate, citric acid and many commercial retardants utilized in the cement industry are suitable. These retardants can be present in weight percent's of between 0.1 to 5 weight percent of the total ceramic mixture, up to 2 weight percent in a preferred concentration, and between 0.5 and 1 weight percent in a most preferred range.

Wagh (2004) citing a study (Sarkar, 1990) on the kinetics of retardation of MgO and ammonium phosphate with boric acid, reported that boric acid develops a polymeric coating on MgO grains which is a less soluble compound preventing the grains from dissolving in the acid solution. Subsequently, as the pH of the solution rises, the coating dissolves slowly into the solution exposing the grains to the acid solution. Therefore dissolution of MgO is delayed and setting is retarded (Wagh, 2004). Wilson et al. (2005) mention that sodium tripolyphosphate (STPP) or borax may be added to retard the MgO and acid salt reaction and reported that the addition of 1.0 to 7.0 % STPP acted as a retarder and increased compressive strength. They also noted that the presence of aluminum in phosphoric acid solution serves to retard the setting reaction.

CHAPTER 3

EXPERIMENTS

3.1 Materials and Characterization

3.1.1 Fly ash

The fly ash sample was obtained from Afşin-Elbistan A power plant, located in Kahramanmaraş, Turkey. It has a brownish gray color with white particles inside. The density of Afşin-Elbistan (AE) fly ash density is 2.41 g/cm^3 determined according to ASTM C188 (2014). The blaine fineness of AE fly ash is determined as 1800 cm^2/g with an air permeability apparatus in accordance with ASTM C204, (2014) . Figure 3.1 shows scanning electron microscopy (SEM) images of AE fly ash.

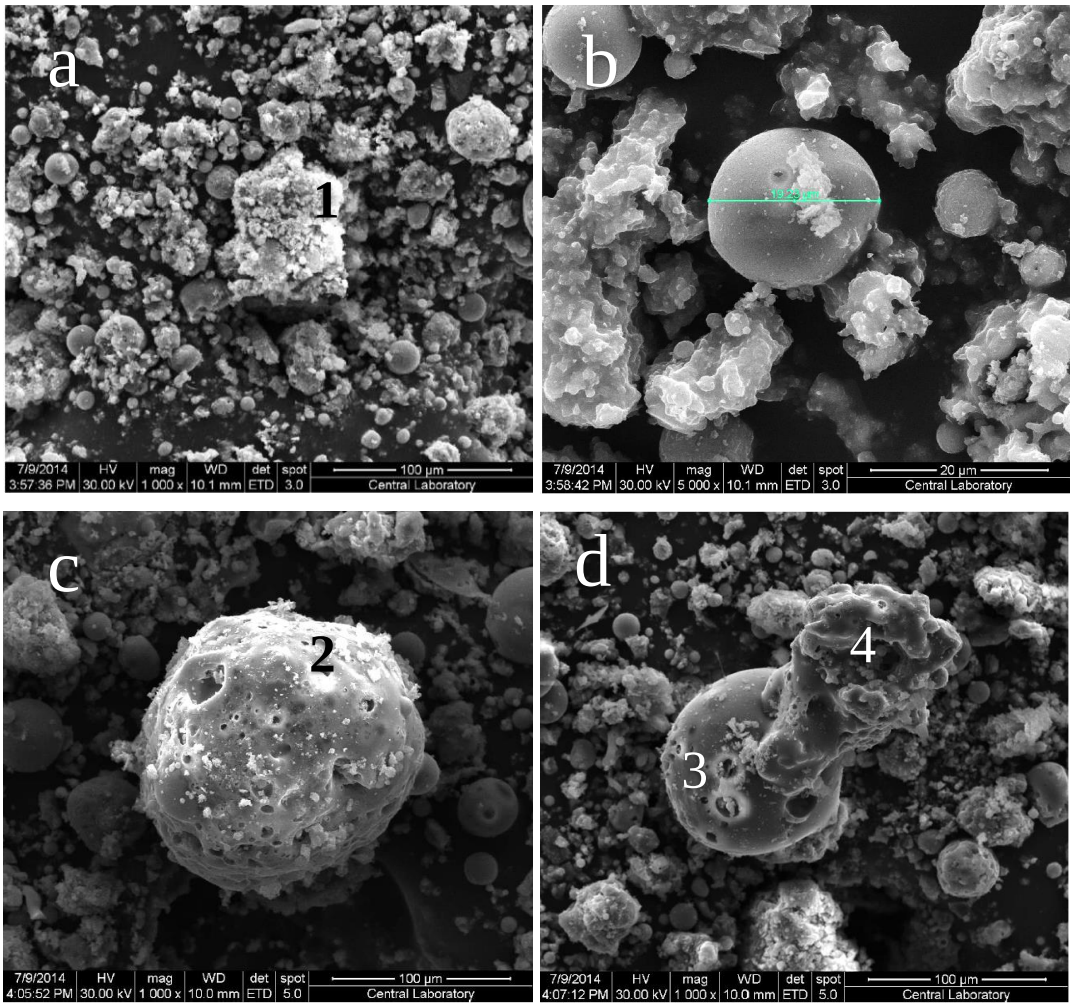

Figure 3.1 SEM images of AE fly ash particles.

Energy dispersive x-ray analysis (EDX) results from various points in the SEM were used to characterize compositions of different particles. The results are exhibited in Table 3.1. X-ray fluorescence analysis (XRF) was performed for identification of AE fly ash chemical components. Table 3.2 gives these results. From Figure 3.1 it is seen that the most of particles are spherical shape with approximate diameters of 1 µm to 100 µm. It was observed that bigger particles have greater visible porosity than the smaller ones. From EDX results it is deduced that particles are similar in consisting elements. Carbon is observed among the elements. This can be because

of unburnt carbon existing in the AE fly ash. Although as previously mentioned, there were white particles observable with bare eye. The presence of sulfur can reveal the nature of these white particles as calcium sulphate ($CaSO_4$). In addition, XRF detected CO_2, which can be liberated from calcium carbonate coming from unburnt coal.

Table 3.1 EDX results of AE fly ash from SEM investigation.

Element	Points from Figure 3.1 that EDX analysis were performed (weight %)			
	1	**2**	**3**	**4**
O	34.62	49.60	26.69	32.91
Mg	1.81	1.29	0.84	0
Al	6.07	13.14	6.48	3.14
Si	10.83	25.14	13.06	5.89
S	5.23	1.54	0	2.63
Ca	36.97	5.73	25.35	43.73
Fe	4.48	2.43	8.74	11.70
C	0	0	15.39	0

Table 3.2 Oxide composition of AE fly ash XRF result.

Component	Oxide amount (weight %)
SiO_2	19.40
CaO	33.30
Al_2O_3	9.50
Fe_2O_3	5.64
MgO	1.88
SO_3	12.90
B_2O_3	5.65

Table 3.2 (continued).

CO_2	9.42
P_2O_5	0.41
K_2O	0.68
TiO_2	0.60
V_2O_5	0.08
Cr_2O_3	0.07
MnO	0.05
NiO	0.02
CuO	0.007
ZnO	0.014
As_2O_3	0.007
Rb_2O	0.004
SrO	0.056
ZrO_2	0.018
Na_2O	0.226

3.1.2 Glass powder

Glass is a rich source of various oxides such SiO_2, CaO, Al_2O_3, Fe_2O_3, etc. and the classification of glasses are in accordance with these oxides. Acids can possibly attack to these oxides causing the migration of the liberated ions to an aqueous phase (Wilson and Nicholson, 2005). In this study brown beer bottles were selected as a source of glass. Beer bottles were crushed and washed with water and oven dried for 24 h at 105 ˚C. They were pulverized in a ball mill for 5 h so that 95 wt % passed a 45 μm sieve. The glass powder produced from dark brown bottles had a grayish white color. According to ASTM C188, (2014), its density was determined 2.52 g/cm^3. The surface area has determined 4200 cm^2/g in accordance with ASTM C204, (2014). XRF revealed the glass powder oxide compositions given in Table 3.3. The high content of Na_2O and CaO, after SiO_2 classified this material as a soda lime glass type.

Table 3.3 Oxide composition of the glass used.

Component	Oxide amount (weight %)
SiO_2	63.3
CaO	10.8
Al_2O_3	1.93
Fe_2O_3	0.64
MgO	2.51
SO_3	0.01
B_2O_3	2.19
CO_2	4.35
P_2O_5	0.02
K_2O	0.49
TiO_2	0.07
Cr_2O_3	0.15
MnO	0.02
ZnO	0.005
SrO	0.01
ZrO_2	0.02
Na_2O	13.4

3.1.3 Calcium Aluminate Cement

Calcium aluminate cement (CAC) is a hydraulic binder which is well known for being rich in Al_2O_3 and CaO contents. The CAC used in this study was provided by Çimsa Production and Trade Co., Turkey under the commercial name "Isıdaç 40". According to manufacturer, this cement has a density of 3.25 g/cm^3 and its surface area is equal to 3000 cm^2/g. Table 3.4 exhibits CAC oxide contents.

Table 3.4 Oxide compositions of the calcium aluminate cement used.

Oxide amount	Oxide amount (weight %)
SiO_2	3.60
CaO	36.20
Al_2O_3	39.80
Fe_2O_3	17.05
MgO	0.65
SO_3	0.01
Na_2O	0.16

3.1.4 Orthophosphoric acid (H_3PO_4)

Orthophosphoric acid is an inorganic mineral acid with the formula H_3PO_4 which is also known as phosphoric acid. It has a molar mass of H_3PO_4 is 97.995 g/mol. An 85 wt% phosphoric acid solution with a density of 1.68 g/cm^3 was used to prepare the solutions with various concentrations used in this study. Table 3.5 gives the molar mass, pH value and density of phosphoric acid with different solution concentrations, at 25˚C (Christensen and Reed, 1955).

3.1.5 Monopotassium dihydrogen phosphate (KH_2PO_4)

Monopotassium phosphate is an acid salt produced by the action of phosphoric acid on potassium carbonate. It is most used as a fertilizer where the soil needs potash. It is a water soluble salt with a molar mass of 136.086 g/mol. Wagh (2004) reported that KH_2PO_4 is the most useful raw material in the production of objects of large size or in a continuous production process and it can produce better ceramics in comparison with other phosphate salts. The KH_2PO_4 used in this study was 99 % pure white crystals. To enhance its solubility, it was pulverized to reach a fineness of 2500 cm^2/g.

Table 3.5 Dilution chart of phosphoric acid (Christensen and Reed, 1955).

Phosphoric acid (H_3PO_4)			
Concentration (%)	molarity	pH	Density of phosphoric acid at 25 °C (g/ml)
10	1.07	1.08	1.05
15	1.66	0.98	1.08
20	2.27	0.91	1.11
25	2.92	0.86	1.15
30	3.61	0.81	1.18
35	4.34	0.77	1.22
40	5.11	0.73	1.25
45	5.93	0.70	1.29
50	6.80	0.67	1.33
55	7.73	0.64	1.38
60	8.71	0.61	1.42
65	9.75	0.59	1.47
70	10.86	0.56	1.52
75	12.04	0.54	1.57
80	13.29	0.52	1.63
85	14.61	0.50	1.68

3.2 Mixture preparation

3.2.1 Mixing procedure

All samples were prepared by mixing an aqueous phosphoric acid or some acid salt with the AE fly ash in the desired liquid/powder ratios. This was been done in two different ways for acid solutions and acid salts.

3.2.1.1 Mixing procedure (acid solutions)

A cylindrical plastic container with both 10 cm diameter and height, isolated with 4 mm rubber shield was used to prepare the mixtures. Stirring was done by hand, with a 5 cm metal blade spatula, at moderate speed to reach a homogenous mixture in one minute. For the solution-to-powder ratios used for the mixtures preparation (S/P = 0.5, 0.6, 0.7, 0.8, 0.9, 1.0, 1.1 and 1.2) the produced mixtures were more similar to dry fine-sand accumulation instead of a workable slurry which can be experienced in Portland cement mixtures. Furthermore the consistency of mixtures did not change sensibly by increasing solution-to-powder ratio at the defined range. Therefore to overcome this low workability, the placement of mixture were performed in two equal layers and each layer was compacted by a tamper (cross section = 20 x 5 mm) 16 times. Tamping pressure was adjusted to ensure uniform filling of each layer.

In the other hand, the mixtures were set in just seconds in the lack of retarder, so for speeding up the molding procedure, for each specimen, separate batches were prepared to keep the mixing and molding time constant for all of the samples.

3.2.1.2 Mixing procedure (acid salt)

When acid salt was used, a planetary electrical mixer used for preparing mixtures. First, the water and acid salt were stirred at low speed for 2 minutes and then the powder was added gently in a period of 30 second to the batch. Finally it was stirred for 7.5 minutes at moderate speed. The workability of acid salt activated mixtures was adequate to easily placed in mold, therefore the molding of these mixtures were performed as acid activated mixtures without needing to high pressure manual compaction.

3.2.2 Powder blends

In this study AE fly ash was selected to be utilized as a major component for phosphate bonded cement production. Glass powder (GP) and calcium aluminate cement (CAC) were also investigated to be used for partial replacement of AE fly ash. Table 3.6 shows the proportions of the various mixtures made.

Table 3.6 Powders used for CBPC production.

		Fly ash	Glass Powder	CAC
control	mix 1	100%	0%	0%
Group A	mix 2	90%	10%	0%
	mix 3	80%	20%	0%
	mix 4	70%	30%	0%
	mix 5	60%	40%	0%
Group B	mix 6	90%	0%	10%
	mix 7	80%	0%	20%
	mix 8	70%	0%	30%
	mix 9	60%	0%	40%
Group C	mix 10	90%	5%	5%
	mix 11	80%	10%	10%
	mix 12	70%	15%	15%
	mix 13	60%	20%	20%
	mix 14	50%	25%	25%
	mix 15	40%	30%	30%
	mix 16	30%	35%	35%
	mix 17	20%	40%	40%
	mix 18	10%	45%	45%
	mix 19	0%	50%	50%

3.2.3 The solution concentration and solution-to-powder ratios used

In hydraulic cements, water is the major solvent. Water has two main roles in hydraulic cement mixtures. Depending on the composition of cement, it participates in the hydration process and the excess water acts as a plasticizer to combine the ingredients and provide workability. The solution used in acid base cements is an acid. In an acid-base cement, where the base is one side of the reaction, acid as a solution, not only makes the paste, but is also responsible for solving the anions by means of providing the necessary pH and providing cations to make the acid-base reaction. Therefore pH and ions in solution is vital for producing a suitable final product. In order to determine the desired equilibrium between these factors, combinations of 30 wt%, 40 wt%, 50 wt%, 60 wt% and 70 wt% diluted phosphoric acid with solution-to-powder ratios of 0.5, 0.6, 0.7, 0.8, 0.9, 1.0, 1.1 and 1.2 were investigated. Since the acid solution is made of dissolving phosphoric acid in water, the accurate water-to-powder ratio were given in Table 3.7.

Table 3.7 Water-to-powder ratio of mixtures.

		Phosphoric acid concentration (wt %)				
		30	40	50	60	70
solution-to-powder ratio	0.5	0.35	0.30	0.25	0.20	0.15
	0.6	0.42	0.36	0.30	0.24	0.18
	0.7	0.49	0.42	0.35	0.28	0.21
	0.8	0.56	0.48	0.40	0.32	0.24
	0.9	0.63	0.54	0.45	0.36	0.27
	1.0	0.70	0.60	0.50	0.40	0.30
	1.1	0.77	0.66	0.55	0.44	0.33
	1.2	0.84	0.72	0.60	0.48	0.36

3.3 Experiments

3.3.1 Mechanical tests

A compressive strength test was performed on the CBPCs. 50 x 50 x 50 mm cube samples. For every age, two samples were cast and for each sample, separate batch was prepared. They were kept at ambient temperature (21±1 ˚C and 35±5% humidity). The universal testing machine used for cube samples crush was a UTEST instrument with a ultimate capacity of 250 KN and a pace rate of 1.5 kN/s was applied.

3.3.1.1 Phosphoric acid concentration and the influence of solution-to-powder ratio

Combination of 30 wt%, 40 wt%, 50 wt%, 60 wt% and 70 wt% phosphoric acid concentrations with solution-to-powder ratio equal to 1, 1.1 and 1.2 were investigated to study the influence of acid concentration on the AE fly ash. 25 combinations (Table 3.7) were used. The samples were tested at 24 h age.

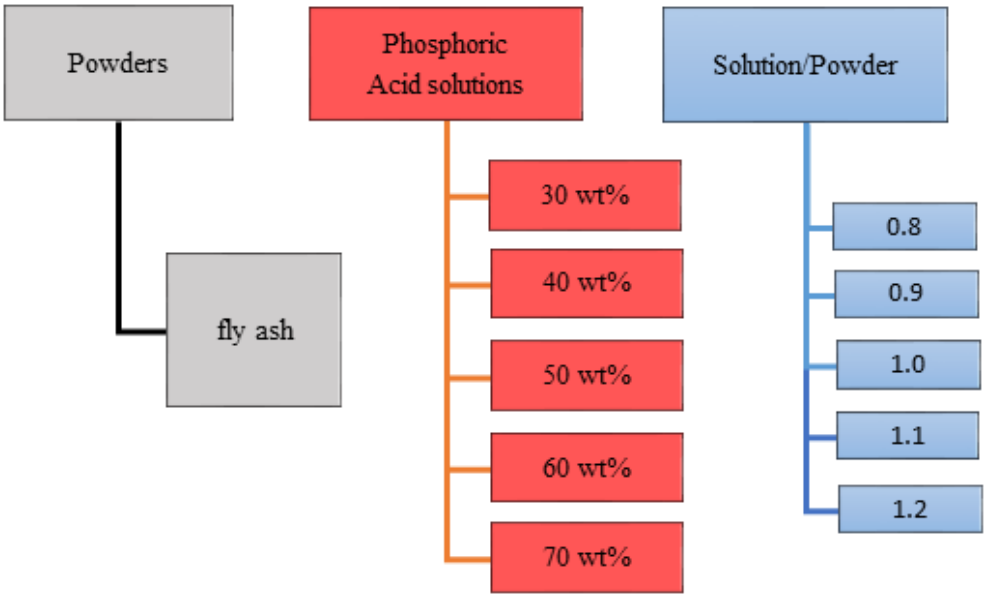

Figure 3.2 25 combinations of various acid concentrations and solution-to-powder ratios.

3.3.1.2 Influence of partial powder replacement

To better understand the influence of partial replacement of the powder, this experiment was divided to two parts:

a) Phosphoric acid concentration and solution-to-powder ratio were kept constant (60 wt% phosphoric acid and solution/powder = 1) and 19 various combinations of powders consist of fly ash, glass powder and CAC (Table 3.6) were utilized to prepare CBPCs samples and their compressive strengths were investigated.
b) Only three combinations of powders were selected to study the influence of various acid concentrations and solution-to-powder ratios. Figure 3.3 has shown the different combinations were used.

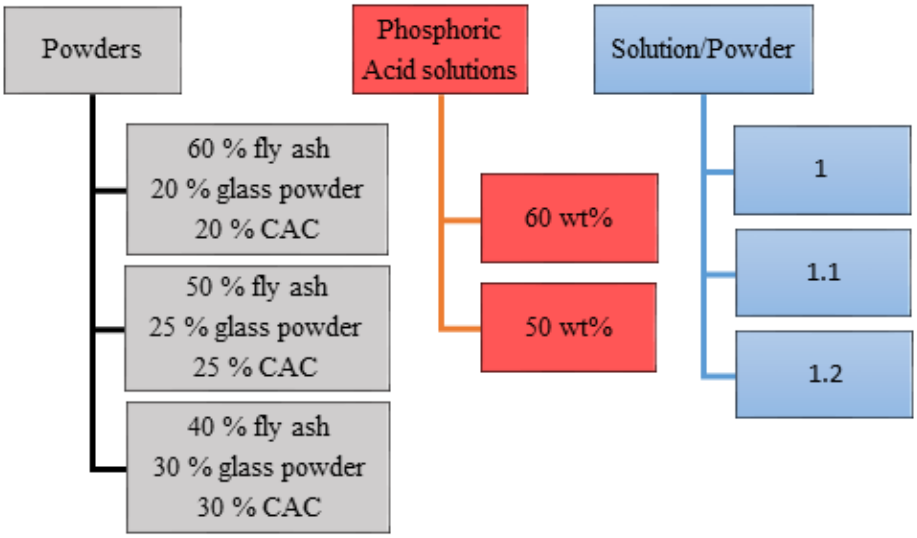

Figure 3.3 Combination of selected powders for inspection of acid concentration and solution-to-powder ratio for compression strength.

3.3.1.3 Increase in strength with time

As previously mentioned, strength development of CBPCs can be very rapid and they can gain a significant portion of their strength in the first hours after forming. To understand the continuation of reaction and the rate of strength increase with time, 28-day strengths were measured for fly ash mixtures with 5 solution-to-powder ratios between 0.5 and 1 and three different concentrations (40 wt%, 50 wt% and 60 wt%) (Figure 3.4). In addition, two powder combinations were selected to investigate their strength increase rate with time as well. Figure 3.5 shows the selected combinations.

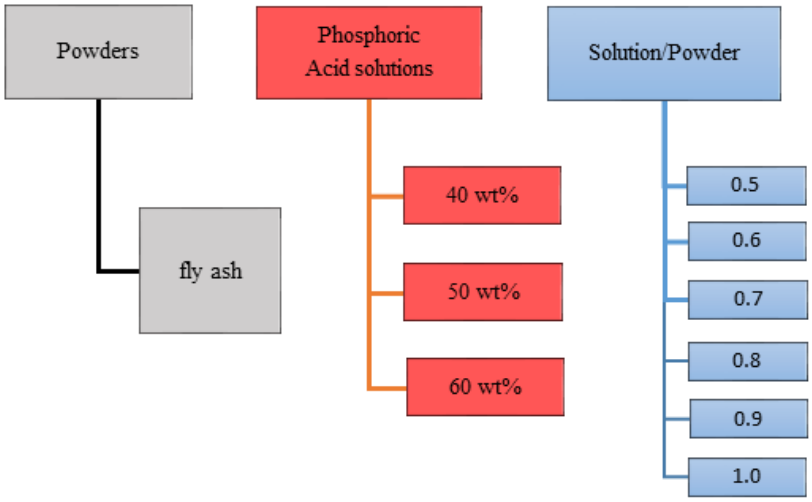

Figure 3.4 18 combinations used to study compressive strength increase with time for the various acid concentrations and solution-to-powder ratios.

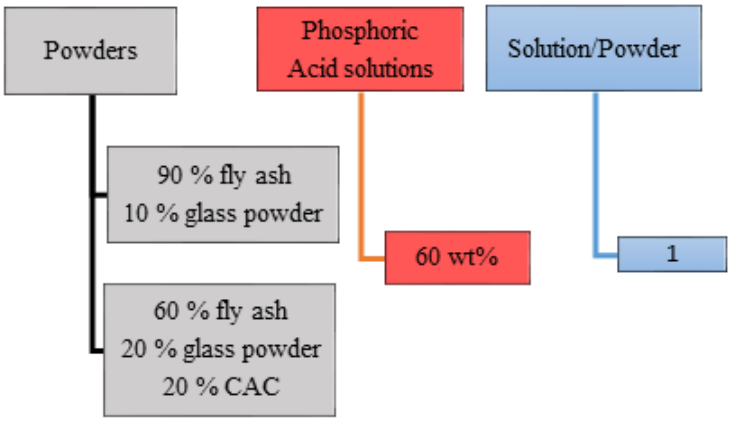

Figure 3.5 Two powder combinations selected for studying the strength increase with time.

3.3.1.4 The Influence of retarder use

Disodium tetraborate decahydrate with the chemical formula of $Na_2B_4O_7 \cdot 10H_2O$ was selected as an additive to the acid solution for the purpose of retarding the reaction, in order to obtain a controlled reaction to reach improved CBPCs products. It was used at four different dosages (0.5 wt%, 1 wt%, 2 wt% and 4 wt% of total powder). All four mixtures were prepared with the 60 wt% phosphoric acid solution and the solution-to-powder ratio of 1.0 (Figure 3.6).

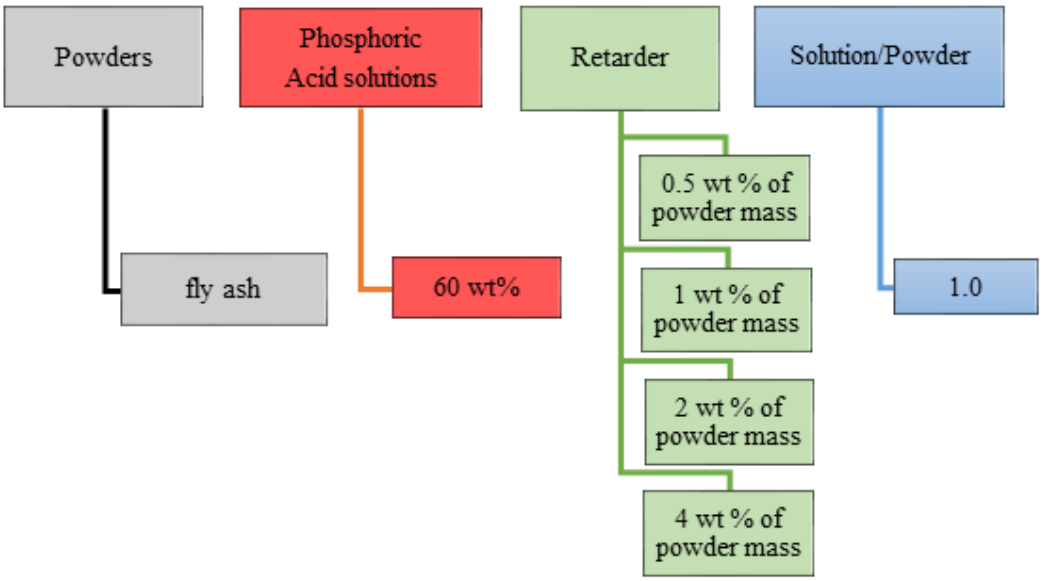

Figure 3.6 Four combinations for studying influence of retarder.

3.3.1.5 The influence of sand addition on the compressive strength

To investigate the binding properties of phosphoric acid solution and the AE fly ash mixture, as an acid-base cement, sand was added to mixture to produce mortar specimens. Samples strength were measured up to 28 days to study the cubic mortar specimen's compressive strength. Three different proportions of sand were used. Figure 3.7 shows the proportions of the mixtures used. The utilized sand was in accordance with EN 196-1 standard.

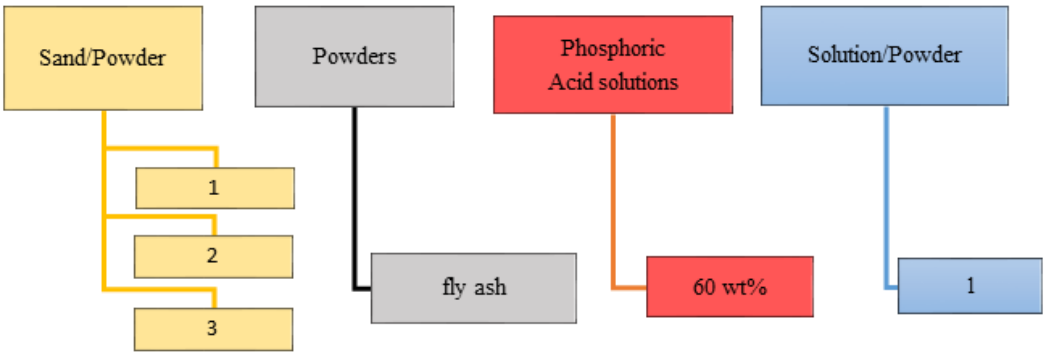

Figure 3.7 Three combinations of sand addition for studying influence of mortar.

3.3.1.6 Influence of acid salt on producing CBPCs

KH_2PO_4 was used as the source of phosphate ions source. To be able to compare the results of the samples produced using acid salt with those produced using phosphoric acid, corresponding proportions of 30 wt%, 40 wt%, 50 wt%, 60 wt% and 70 wt% phosphoric acid solutions (Figure 3.8), were prepared by KH_2PO_4 by considering the provided phosphate ions (Equation 3.1). In addition, the mixtures were prepared with an amount of water equal to the water containing contribution of corresponding acid solutions (Equation 3.2).

Table 3.8 Phosphate content of H_3PO_4 and KH_2PO_4.

	Molar mass ($g.mol^{-1}$)	phosphate ion contained
H_3PO_4	97.99	(94.97/97.99)*100 = 96.92%
KH_2PO_4	136.08	(94.97/136.08)*100 = 69.79%
PO_4^{3-}	94.97	

$$M_s = M_a * C * \frac{96.92\%}{69.79\%} \quad (3.1)$$

where:

M_s, is the mass of the acid salt (g)

M_a, is the corresponding mass of the phosphoric acid solution (g)

C, is the corresponding concentration of the phosphoric acid (%)

$$W = M_a * (100 - C) \quad (3.2)$$

where:

W is the water content contribution of phosphoric acid solution (g)

M_a and C are as Equation 3.1

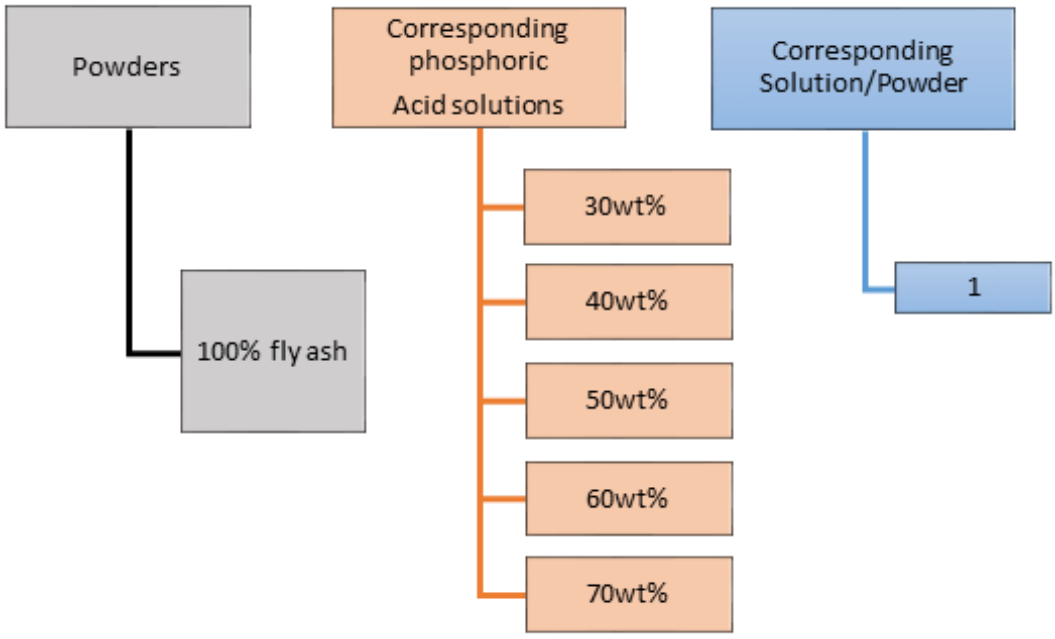

Figure 3.8 Five combinations of various acid salt concentrations for studying the influence of KH_2PO_4 on producing CBPC.

3.3.1.7 Influence of combination of H_3PO_4 and KH_2PO_4

In this step, the compressive strengths of samples prepared with constant amount of PO_4^{-3} anions, were evaluated. The anions in this experiment had been provided with various combinations of acid solutions and acid salts. Solution-to-powder ratio for all of the mixtures, was fixed 1.0. Table 3.9 shows the combinations used.

Table 3.9 Five combinations of studying H_3PO_4 and KH_2PO_4 contribution influence.

no.	Powder	Acid salt	Acid	water
combination 1	AE Fly Ash	0% of PO_4^{3-} ion by solid KH_2PO_4	100% of PO_4^{3-} ion by 60 wt% H_3PO_4	no water was added
combination 2	AE Fly Ash	25% of PO_4^{3-} ion by solid KH_2PO_4	75% of PO_4^{3-} ion by 60 wt% H_3PO_4	The water content contribution of the 25% excluded acid
combination 3	AE Fly Ash	50% of PO_4^{3-} ion by solid KH_2PO_4	50% of PO_4^{3-} ion by 60 wt% H_3PO_4	The water content contribution of the 50% excluded acid
combination 4	AE Fly Ash	75% of PO_4^{-3} ion by solid KH_2PO_4	25% of PO_4^{-3} ion by 60 wt% H_3PO_4	The water content contribution of the 75% excluded acid
combination 5	AE Fly Ash	100% of PO_4^{3-} ion by solid KH_2PO_4	0% of PO_4^{3-} ion by 60 wt% H_3PO_4	The water content contribution of the 100% excluded acid

3.3.2 Mixtures pH evaluation

To study the influence of pH on the formation of CBPCs, 18 pastes were prepared combining phosphoric acid and potassium dihydrogen phosphate. The concentrations of solution were 50 wt%, 60 wt% and 70 wt% for acid and corresponding concentrations for acid salt. Solution-to-powder ratios equal to 0.8, 1 and 1.2 were selected for paste preparation. The first pH measurement was done when the mixture was still a slurry. After hardening, the paste were ground in a manual grinder to pass a 200 μm sieve. Thereafter, 10 g of powder and 10 g of distilled water were weighed with an accuracy of 0.1 g and mixed together by using a magnetic mixer at moderate speed for one minute. After mixing, the suspension was poured into a test tube and its pH was measured. An “Okton waterproof 300 series” pH meter was used.

3.3.3 Isothermal calorimetry

Isothermal calorimetry measures heat flux using specific sensors inside a chamber at constant temperature. Calorimetry experiments were done using a TAM Air Isothermal Calorimeter. Heat of reaction was measured in time with an in-situ mixing equipment for both phosphoric acid and potassium dihydrogen phosphate mixtures. In this experiment series, the AE fly ash was exposed to three various concentrations of 40 wt%, 50 wt% and 60 wt% phosphoric acid solutions with solution-to-powder ratios equal to one. In addition, corresponding concentrations and solution-to-powder ratio were considered for acid salt utilization. Each sample was monitored continuously 168 h.

3.3.4 Scanning Electron Microscopy (SEM)

Scanning electron microscopy (SEM) was performed using a "Feiquanta-400F" microscope at the METU Central Laboratory. Surface topographies of the solid samples were generally studied. SEM images were obtained from the AE fly ash as study main raw material, and several produced CBPCs listed in Table 3.10. To see the microstructure, 60-day old sample pastes were broken and a piece from inner parts was selected for SEM examination. Samples were oven dried at 80 ˚C for 24 hours and then gold-palladium coated in a high-pressure vacuum.

Table 3.10 CBPC samples investigated using SEM.

Sample	Powder	Solution	Solution / Powder
1	Fly ash	-	-
2	Fly ash	60 wt% H_3PO_4	1
3	Fly ash	KH_2PO_4 (~ 60 wt% H_3PO_4)	(~1)
4	Fly ash	60 wt% H_3PO_4 + 0.5 % Retarder	1
5	90% Fly ash + 10% Glass	60 wt% H_3PO_4	1
6	60% Fly ash + 20% Glass powder + 20% CAC	60 wt% H_3PO_4	1

Elemental analysis is commonly used in conjunction with SEM imaging. The basis of the technique lies in the emission of X-rays from the surface of materials upon exposure to a primary beam of electrons of suitable energy. The energy of the X-ray emission is measured by energy dispersive spectrometry (EDX/EDS) detectors providing qualitative and quantitative information can be obtained from the some portion of the sample under direct microscopic observation (Rossiter et al., 1991). It was performed on several regions of the fly ash particle (Table 3.1) and paste samples as well.

3.3.5 X-ray Fluorescence analysis (XRF)

X-Ray Fluorescence analysis (XRF) is an analytical technique that uses the interaction of x-rays with a material to determine its elemental composition. A "Rigaku ZSX Primus II" XRF device was used at the METU Central Laboratory to characterize raw materials used. The presence of elements from Boron to Uranium was inspected. Table 3.2, Table 3.3 and Table 3.4 show the oxide compositions of the AE fly ash, the glass used and the CAC used.

3.3.6 X-Ray Diffraction (XRD)

Powder X-ray Diffraction (XRD) is the most accurate and powerful technique of both identifying solids and determining their structures. A "Rigaku Ultima-IV" XRD instrument was used to characterize the structures of the solid raw materials and those of the final products. All of the samples were scanned from 3˚ to 80˚ at a pace of 0.5 ˚/min. High-sensitively prepared 60-day old pastes were pulverized manually to pass a 100 μm sieve and analyzed.

CHAPTER 4

RESULTS AND DISCUSSION

In this chapter, results obtained from the chemical and structural analysis of raw materials and final products are discussed. Comparisons are made between samples made using different combinations of powders, acid solution concentrations and effective solution-to-powder ratios to obtain a suitable final product.

4.1 Results of compressive strength experiment

4.1.1 The influence of phosphoric acid concentration and solution-to-powder ratio on products strength

24-h compressive strengths of samples with various acid solution concentrations and solution-to-powder ratios, are given in Table 4.1. Figures 4.1 and 4.2 reveal how sample compressive strength is affected by phosphoric acid concentration and content.

Table 4.1 Compressive strength results of 20 combinations for investigating acid concentration and solution-to-powder ratio influence at age 24 h.

	Compressive strength (MPa)				
Acid concentration (wt%)	Solution/ Powder = 0.8	Solution/ Powder = 0.9	Solution/ Powder = 1.0	Solution/ Powder = 1.1	Solution/ Powder = 1.2
30	0.50	0.58	0.69	0.67	0.54
40	1.30	2.80	2.83	2.15	2.76
50	2.60	3.70	4.34	4.38	7.81
60	7.80	13.10	15.50	15.10	12.19
70	2.10	2.40	2.59	2.62	4.55

It is deduced from the results that 60 wt% phosphoric acid solution behaves differently than other solution concentrations. There is a great difference between compressive strength followed with 60 wt% phosphoric acid solutions and those achieved using other concentrations. In addition a solution-to-powder ratio equal to 1.0, seems to give greater values of compressive strength in comparison with other ratios.

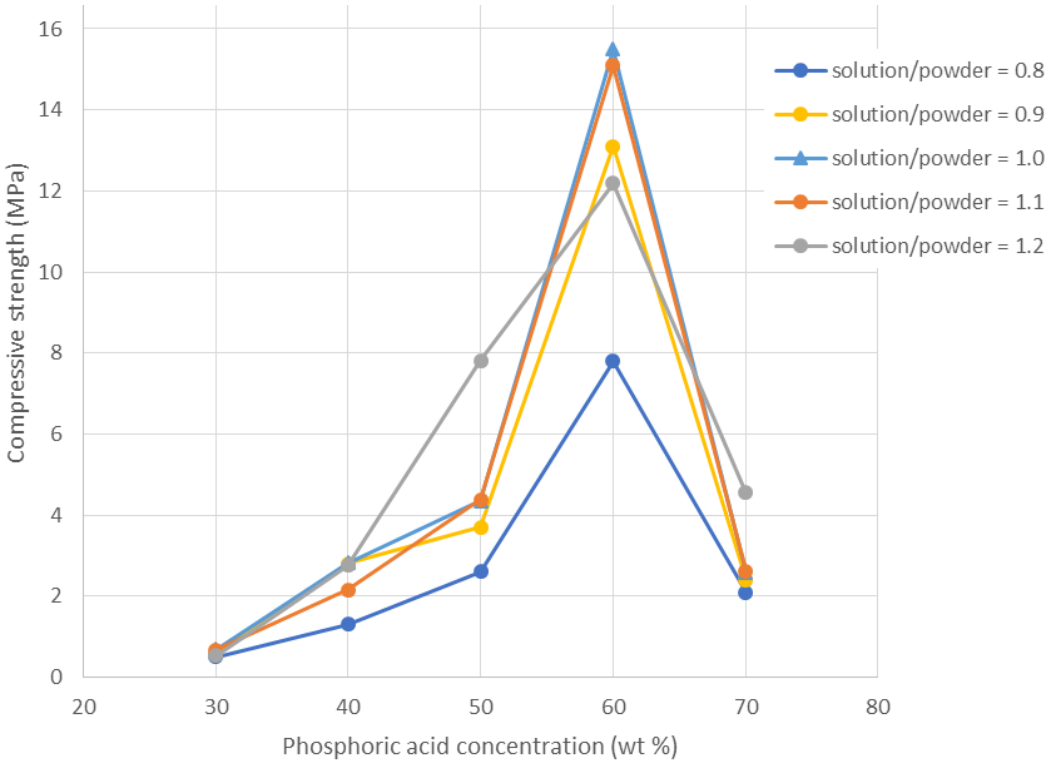

Figure 4.1 Strength development of samples made using various acid concentrations at different solution-to-powder ratios.

4.1.2 Influence of powder partial replacement

Table 4.2 gives the compressive strength of the samples prepared by partially replace AE fly ash with the glass powder and CAC. 60 wt% phosphoric acid was used in these acid-base reactions and the solution-to-powder ratio was kept 1.0.

Table 4.2 Compressive strengths of powder combinations.

	Mix	Powder combination			Phosphoric acid concentration (wt%)	Solution/ Powder	Compressive strength (MPa)
		Fly ash (wt%)	Glass powder (wt%)	CAC (wt%)			
control	1	100	0	0	60	1	15.2
Group A	2	90	10	0	60	1	14.9
	3	80	20	0	60	1	8.6
	4	70	30	0	60	1	4.6
	5	60	40	0	60	1	3.8
Group B	6	90	0	10	60	1	8.1
	7	80	0	20	60	1	6.0
	8	70	0	30	60	1	4.4
	9	60	0	40	60	1	2.4
Group C	10	90	5	5	60	1	10.8
	11	80	10	10	60	1	11.8
	12	70	15	15	60	1	13.2
	13	60	20	20	60	1	15.9
	14	50	25	25	60	1	14.8
	15	40	30	30	60	1	13.2
	16	30	35	35	60	1	12.0
	17	20	40	40	60	1	10.7
	18	10	45	45	60	1	7.5
	19	0	50	50	60	1	4.6

Figure 4.2 shows the graphical evolution of compressive strength result by partial replacement of AE fly ash with glass and CAC. First sample which was prepared with only the AE fly ash, was kept as control sample (gray column). Addition of CAC to the batch (yellow columns) decreases the compressive strength of samples dramatically. Certainly for the glass addition (blue columns) more than 10 % similar results were obtained. Hence the results are different for combined powder replacement of AE fly ash with glass powder and CAC. When 10 wt% of the AE fly ash is replaced (green columns), the compressive strength was dropped in comparison with control sample, but the strength increased as the replacement amount increased, until in mix 13, when 40 wt% of the AE fly ash was replaced with equal weights of glass and CAC. This peak had similar strength with the control sample. Thereafter, with increasing the replacement amount, compressive decreased. Another remarkable mixture is mix 2, where just 10 wt% of the AE fly ash were replaced with glass. It had a slightly lower strength from control sample.

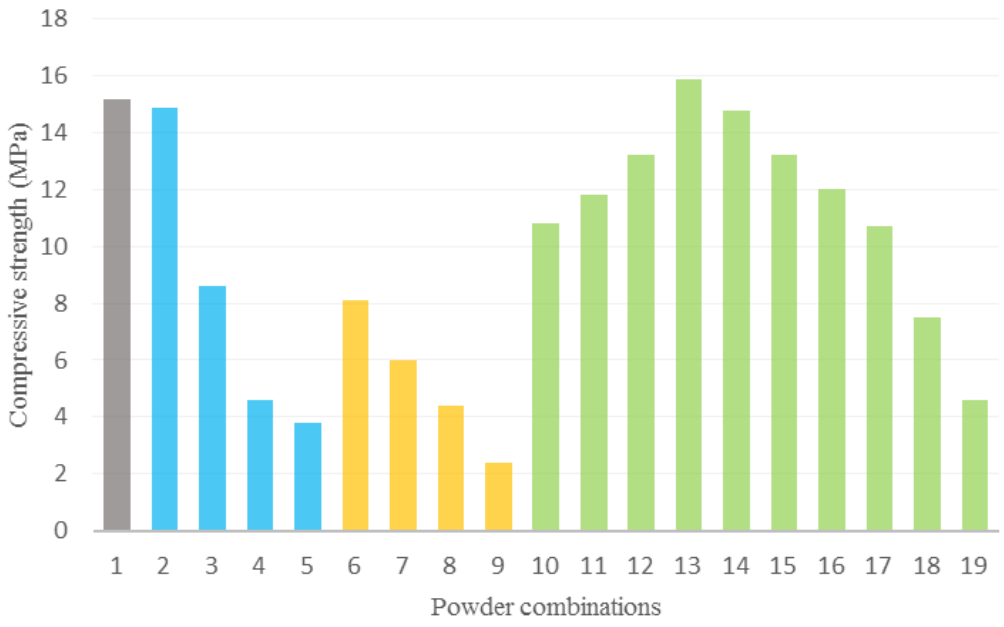

Figure 4.2 Comparison of compressive strengths of various powder combinations.

To better evaluate the influence of the partial fly ash replacement with glass powder or of CAC, three samples (mixes 13, 14 and 15) with higher strength were selected for being studied with different acid solution concentrations and various solution-to-powder amounts. Table 4.3 shows these results.

Table 4.3 Compressive strengths of three selected powder combinations with various acid concentrations and solution-to-powder ratios.

Mix	Fly ash content (wt%)	Glass powder content (wt%)	CAC content (wt%)	Phosphoric acid concentration (wt%)	Solution/ Powder	Compressive strength (MPa)
Mix 13	60	20	20	60	1.0	16.2
Mix 13					1.1	12.6
Mix 13					1.2	8.6
Mix 14	50	25	25		1.0	14.8
Mix 14					1.1	8.0
Mix 14					1.2	7.5
Mix 15	40	30	30		1.0	12.5
Mix 15					1.1	7.0
Mix 15					1.2	6.0
Mix 13	60	20	20	50	1.0	5.5
Mix 13					1.1	5.8
Mix 13					1.2	5.8
Mix 14	50	25	25		1.0	8.0
Mix 14					1.1	5.8
Mix 14					1.2	5.7
Mix 15	40	30	30		1.0	4.8
Mix 15					1.1	3.7
Mix 15					1.2	5.8

Figure 4.3 shows that the 60 wt% phosphoric acid solution exhibited better performance than the 50 wt% solution in 24 h. Although the increase of the solution-to-powder ratio, did not improve the strength of mixtures.

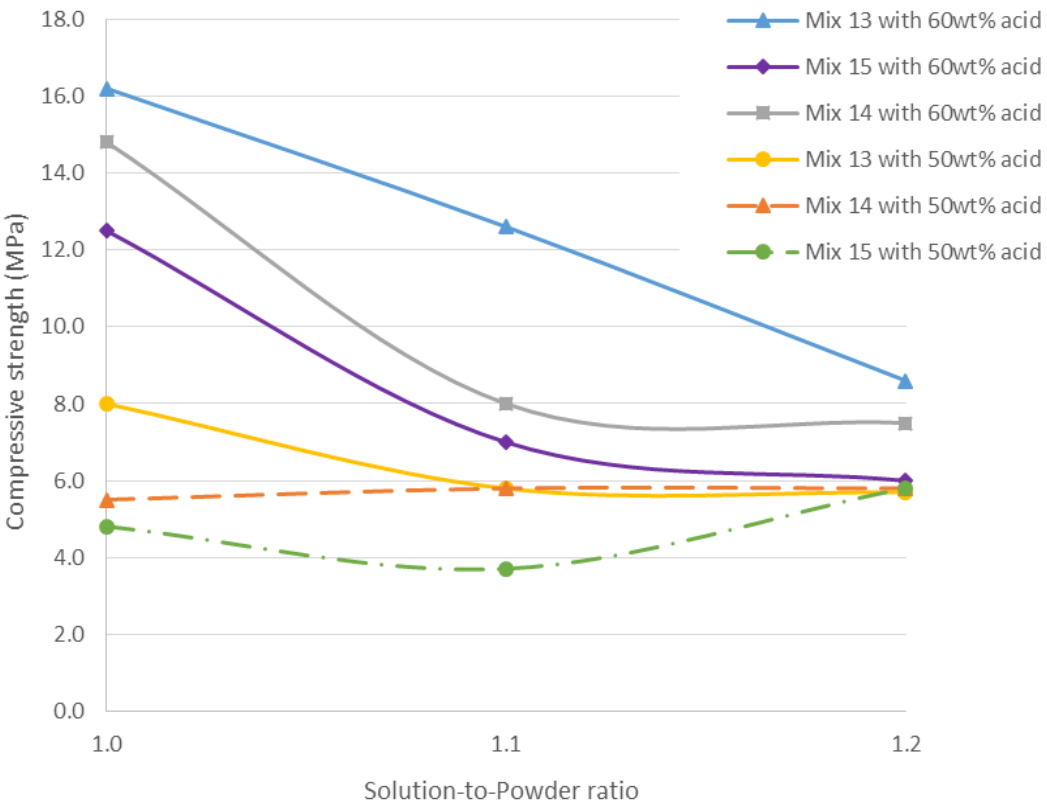

Figure 4.3 Compressive strengths of three selected powder combinations with various acid concentrations and solution-to-powder ratios.

4.1.3 Increase of strength with time

Table 4.4 presents the evolution of compressive strength of the paste samples over a 28-day period. All of the first 18 mixtures use 100 wt% AE fly ash. The last two mixtures (mix 19 and 20) were selected among powder combinations which had exhibited performance similar to 100 wt% AE fly ash.

Table 4.4 Evolution of compressive strength by time.

				Compressive strength (MPa)		
	Solution	Powder	Solution/ powder	1 day	7 days	28 days
mix 1	60 wt% H_3PO_4	Fly ash	1	14.9	20.2	22.1
mix 2	60 wt% H_3PO_4	Fly ash	0.9	13.1	17.1	14
mix 3	60 wt% H_3PO_4	Fly ash	0.8	7.8	10.5	9.2
mix 4	60 wt% H_3PO_4	Fly ash	0.7	2.6	4.4	3.4
mix 5	60 wt% H_3PO_4	Fly ash	0.6	2	2.7	1.7
mix 6	60 wt% H_3PO_4	Fly ash	0.5	0.9	1.9	0.5
mix 7	50 wt% H_3PO_4	Fly ash	1	3.1	3.7	2.8
mix 8	50 wt% H_3PO_4	Fly ash	0.9	2.1	2.6	2.3
mix 9	50 wt% H_3PO_4	Fly ash	0.8	2.6	3	2.6
mix 10	50 wt% H_3PO_4	Fly ash	0.7	1.8	2.5	2.2
mix 11	50 wt% H_3PO_4	Fly ash	0.6	1.3	1.6	0.6
mix 12	50 wt% H_3PO_4	Fly ash	0.5	1	1.2	0.2
mix 13	40 wt% H_3PO_4	Fly ash	1	2.2	2.7	2
mix 14	40 wt% H_3PO_4	Fly ash	0.9	1.8	2.2	1.4
mix 15	40 wt% H_3PO_4	Fly ash	0.8	1.3	1.4	0.6
mix 16	40 wt% H_3PO_4	Fly ash	0.7	1.2	1.3	0.6
mix 17	40 wt% H_3PO_4	Fly ash	0.6	0.6	0.7	0.4
mix 18	40 wt% H_3PO_4	Fly ash	0.5	0.4	0.5	0.3
mix 19	60 wt% H_3PO_4	90 wt% Fly ash 10 wt% Glass powder	1	13	24	30
mix 20	60 wt% H_3PO_4	60 wt% Fly ash 20 wt% Glass powder 20 wt% CAC	1	15	20.4	24.8

Two different behaviors can be seen in Figure 4.4, Figure 4.5 and Figure 4.6. All of the mixtures show an increase in compressive strength until age 7 days, but unexpectedly, all mixtures except mixture which was prepared with 60 wt% phosphoric acid solution, decrease in strength from 7 days to 28 days. Strength development continues for only the AE fly ash mixture with a solution-to-powder ratio of 1.0 and was prepared with 60 wt% phosphoric acid solution.

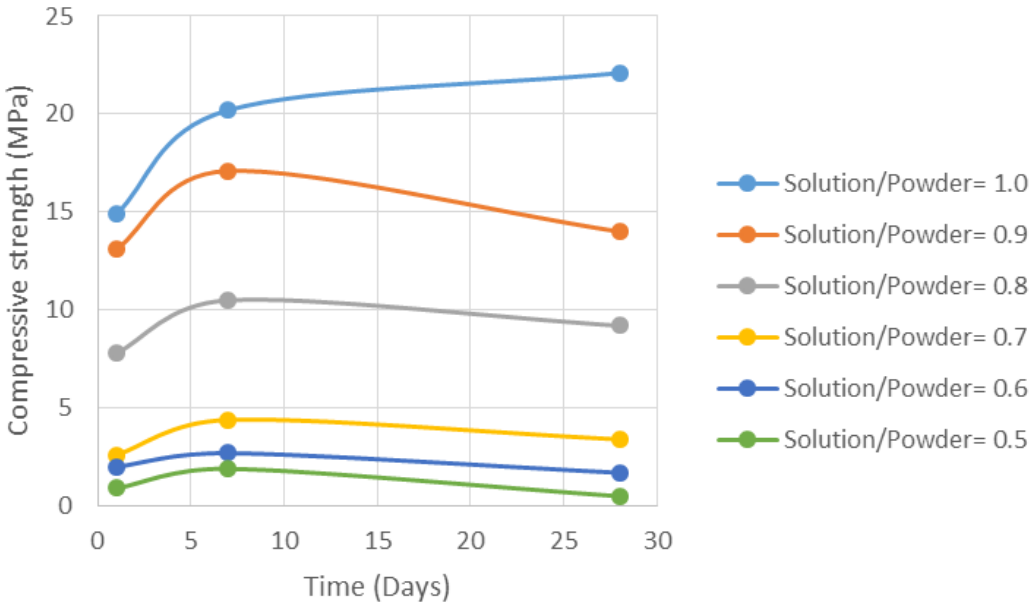

Figure 4.4 Strength evolution in time for samples prepared with 60 wt% phosphoric acid solution.

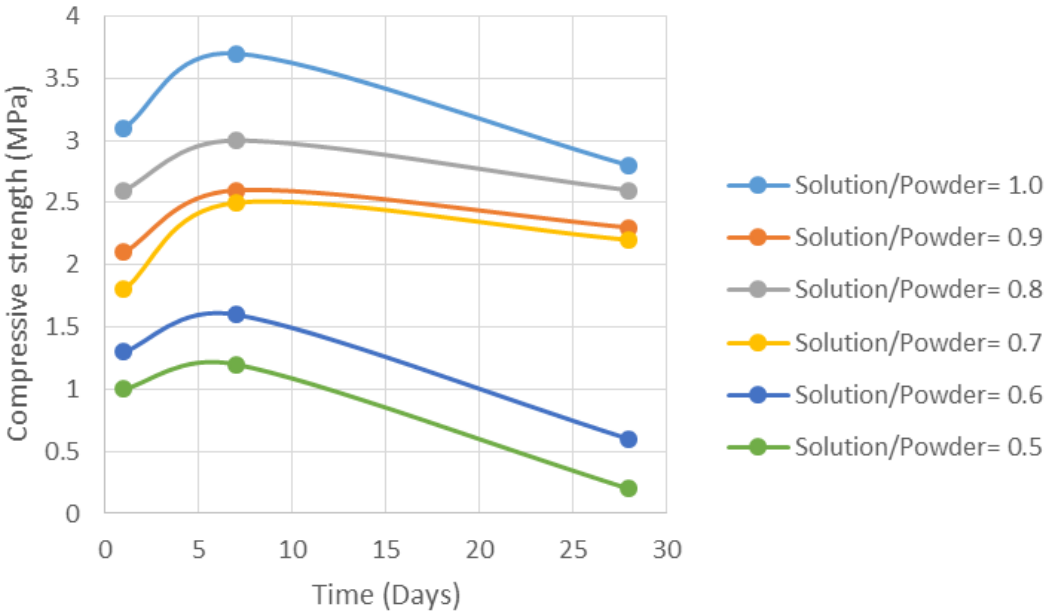

Figure 4.5 Strength evolution with time for samples prepared with 50 wt% phosphoric acid solution.

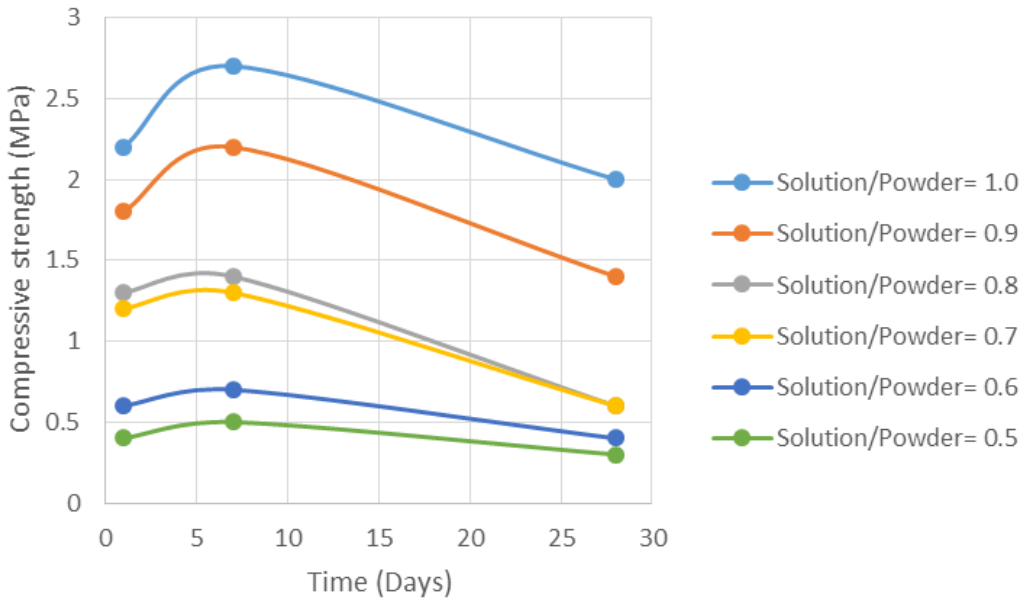

Figure 4.6 Strength evolution with time for samples prepared with 40 wt% phosphoric acid solution.

The inspections of compressive strength growth in time for the two selected powder combinations didn't show the surprising strength loss observed for the previous samples. An even higher 28-days strength was observed to the control mixture. This might be prove that 60 wt% phosphoric acid with solution-to-powder ratio equal to one would be a suitable combination for producing CBPCs with the AE fly ash. In addition, substituting 10 wt% of the AE fly ash with glass powder improved the 28-day compressive strength of the sample, and exhibited 35 % greater strength than the control sample.

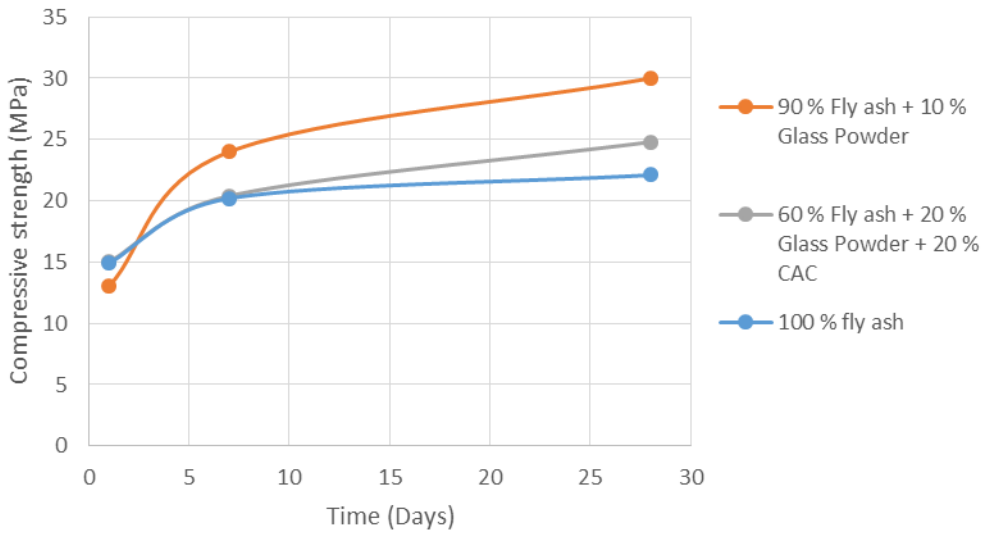

Figure 4.7 Strength evolution of the selected powder combinations in time for 60 wt% phosphoric acid solution.

4.1.4 Influence of retarder

Table 4.5 gives the compressive strength of the AE fly ash CBPCs containing various amounts of di-sodium tetraborate decahydrate ($Na_2B_4O_7 \cdot 10H_2O$). Because of the boron content of this component, as it was expected, the workability of mixtures slightly improved. Figure 4.8 represents that how addition of retarder can affect the strength evolution in formation of CBPCs. Applying 0.5 to 1 % di-sodium tetraborate decahydrate to the mixture, increased the compressive strength of product where addition of more than 1% retarder, significantly decreased it. The tendency for strength loss after 7 days age, was observed again for samples containing 1, 2, and 4 % of retarder.

Table 4.5 Influence of retarder addition on compressive strength of products.

	Mixture materials and properties				Compressive strength (MPa)		
Mix	Solution	Retarder	Powder	Solution / Powder	1 Day	7 Days	28 Days
1	60 w% H_3PO_4	+ 0.5 wt% of powder mass $Na_2B_4O_7 \cdot 10H_2O$	Fly ash	1	23.5	25.8	26.2
2	60 w% H_3PO_4	+ 1 wt% of powder mass $Na_2B_4O_7 \cdot 10H_2O$	Fly ash	1	17.2	25.0	23.1
3	60 w% H_3PO_4	+ 2 wt% of powder mass $Na_2B_4O_7 \cdot 10H_2O$	Fly ash	1	13.0	16.2	13.0
4	60 w% H_3PO_4	+ 4 wt% of powder mass $Na_2B_4O_7 \cdot 10H_2O$	Fly ash	1	8.5	6.9	5.8

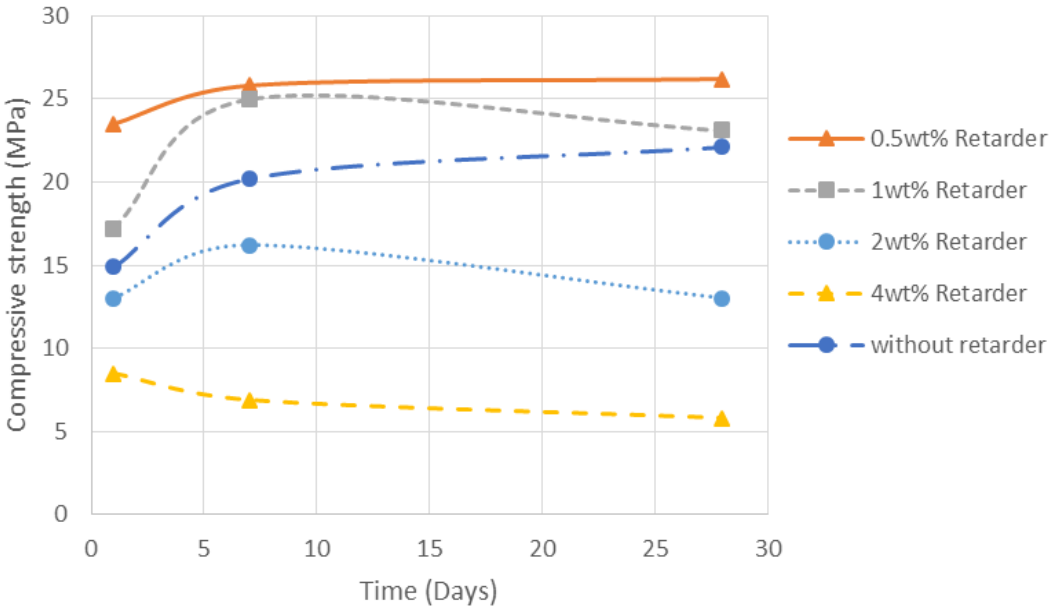

Figure 4.8 Compressive strength evolution of samples containing the retarding chemical.

4.1.5 Influence of sand addition to mixtures

Table 4.6 gives the 1, 7 and 28-day strengths of mortars with different proportions of sand and binder. A decrease in the compressive strength with decreasing binder-to-sand ratio is expected. The mortar mixture consisting of equal masses of the AE fly ash and sand, shows a 50 % decrease in strength, compared with the paste mixture with just fly ash. Figure 4.9 reveals that strength of mortar mixtures with sand-to-powder ratios of 2 and 3 slightly decrease after 7 days. This can be related to the solution absorption of sand particles, to decrease the available acid solution for reaction, and drop the solution to the fly ash ratio lower than one, exhibiting the same behavior with paste samples with solution-to-powder ratios lower than one.

Table 4.6 28-day compressive strength of the mortar samples.

	Mixture materials		Mixture properties		Compressive strength (MPa)		
Mix	Solution	Powder	Solution / Powder	Sand / Powder	1 Day	7 Days	28 Days
1	60 wt% H_3PO_4	Fly ash	1	1	6.1	9.8	11.3
2	60 wt% H_3PO_4	Fly ash	1	2	3.4	4.2	3.9
3	60 wt% H_3PO_4	Fly ash	1	3	1.8	2.6	2.1

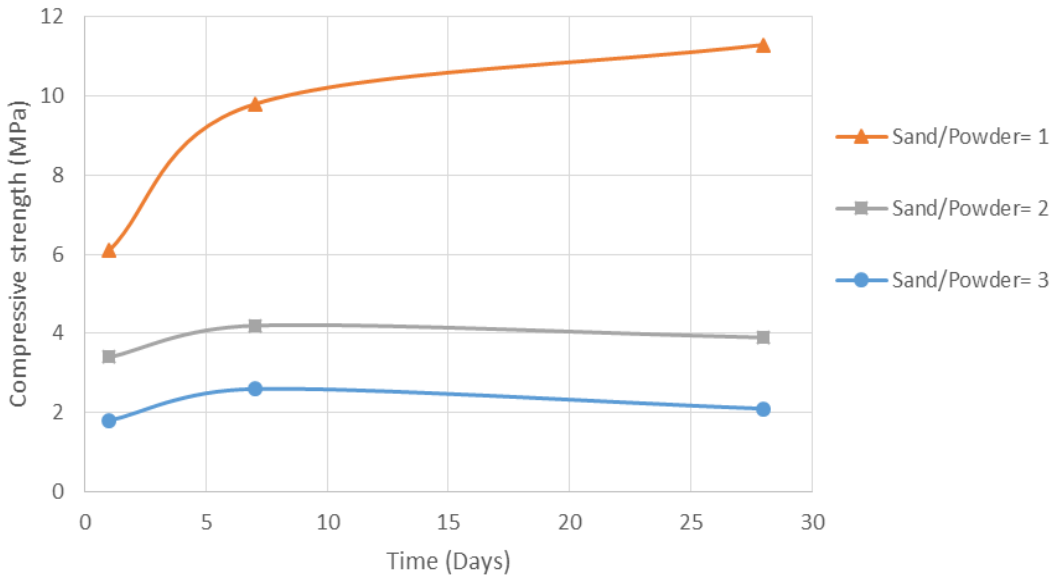

Figure 4.9 The compressive strength evolution of mortar samples.

4.1.6 Influence of acid salt use on CBPCs production

Table 4.7 shows the strengths of paste samples prepared with KH_2PO_4. As can be seen in Figure 4.10, the strength gain continues for 28 days, and the slopes of all curves are positive. Compressive strength increase with increasing the concentration of acid salt is apparent.

Table 4.7 Compressive strengths of paste samples prepared with KH_2PO_4.

Mix	Powders		Compressive strength (MPa)		
			1 Day	7 Days	28 Days
mix 1 containg equivalent phosphate ions and water content with 30 wt% phosphoric acid solution at solution-to-powder ratio equal to 1.0	KH_2PO_4	Fly ash	0.8	1.7	2.1
mix 2 containg equivalent phosphate ions and water content with 40 wt% phosphoric acid solution at solution-to-powder ratio equal to 1.0	KH_2PO_4	Fly ash	1.3	2.7	3.6
mix 3 containg equivalent phosphate ions and water content with 50 wt% phosphoric acid solution at solution-to-powder ratio equal to 1.0	KH_2PO_4	Fly ash	2	4.3	6.1
mix 4 containg equivalent phosphate ions and water content with 60 wt% phosphoric acid solution at solution-to-powder ratio equal to 1.0	KH_2PO_4	Fly ash	3.5	6.5	8.2
mix 5 containg equivalent phosphate ions and water content with 70 wt% phosphoric acid solution at solution-to-powder ratio equal to 1.0	KH_2PO_4	Fly ash	4.1	7.9	9.5

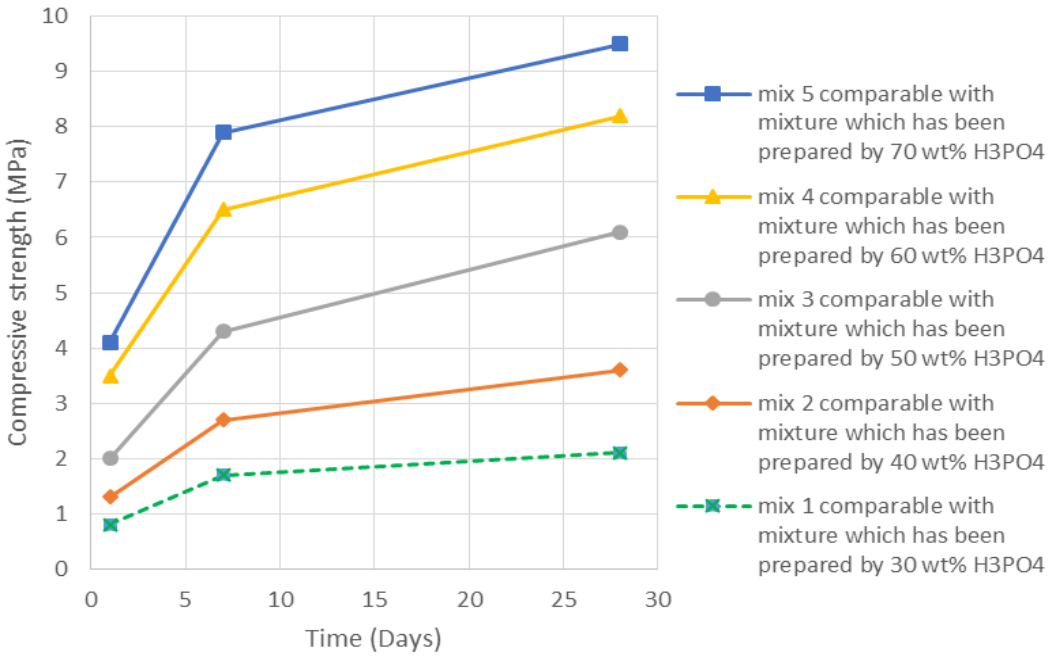

Figure 4.10 Evolution of compressive strength for paste samples prepared with KH_2PO_4.

4.1.7 Influence of combination of phosphoric acid and monopotassium dihydrogen phosphate

Table 4.8 gives the compressive strength of paste samples prepared with the various combinations of the acid and the acid salt, keeping the amount of phosphate ions constant. Figure 4.11 expresses that, the same amount of phosphate ions coming from 60 wt% phosphoric acid produces approximately 2.5 times the strength in comparison with the acid salt, and the strength even drop lower, when a combination of the acid and the acid salt is used for mixture preparation. This can be explicitly express the contribution of other issues such a pH rather than the amount of phosphate ions in CBPC formation.

Table 4.8 Compressive strengths of paste samples prepared with combinations of H_3PO_4 and KH_2PO_4.

	Mixture materials				Compressive strength (MPa)		
Mix	Powder	Acid salt	Acid	water	1 Day	7 Days	28 Days
1	Fly Ash	0 % of PO_4^{3-} ion by solid KH_2PO_4	100 % of PO_4^{3-} ion by 60 wt% H_3PO_4	no water was added	15.0	20.5	22.5
2	Fly Ash	25 % of PO_4^{3-} ion by solid KH_2PO_4	75 % of PO_4^{3-} ion by 60 wt% H_3PO_4	The water content contribution of the 25 % acid excluded	1.5	2.9	2.3
3	Fly Ash	50 % of PO_4^{3-} ion by solid KH_2PO_4	50 % of PO_4^{3-} ion by 60 wt% H_3PO_4	The water content contribution of the 50 % acid excluded	2.5	3.4	4.3
4	Fly Ash	75 % of PO_4^{3-} ion by solid KH_2PO_4	25 % of PO_4^{3-} ion by 60 wt% H_3PO_4	The water content contribution of the 75 % acid excluded	1.1	1.6	3.1
5	Fly Ash	100 % of PO_4^{3-} ion by solid KH_2PO_4	0 % of PO_4^{3-}ion by 60 wt% H_3PO_4	The water content contribution of the 100 % acid excluded	3.5	6.7	8.0

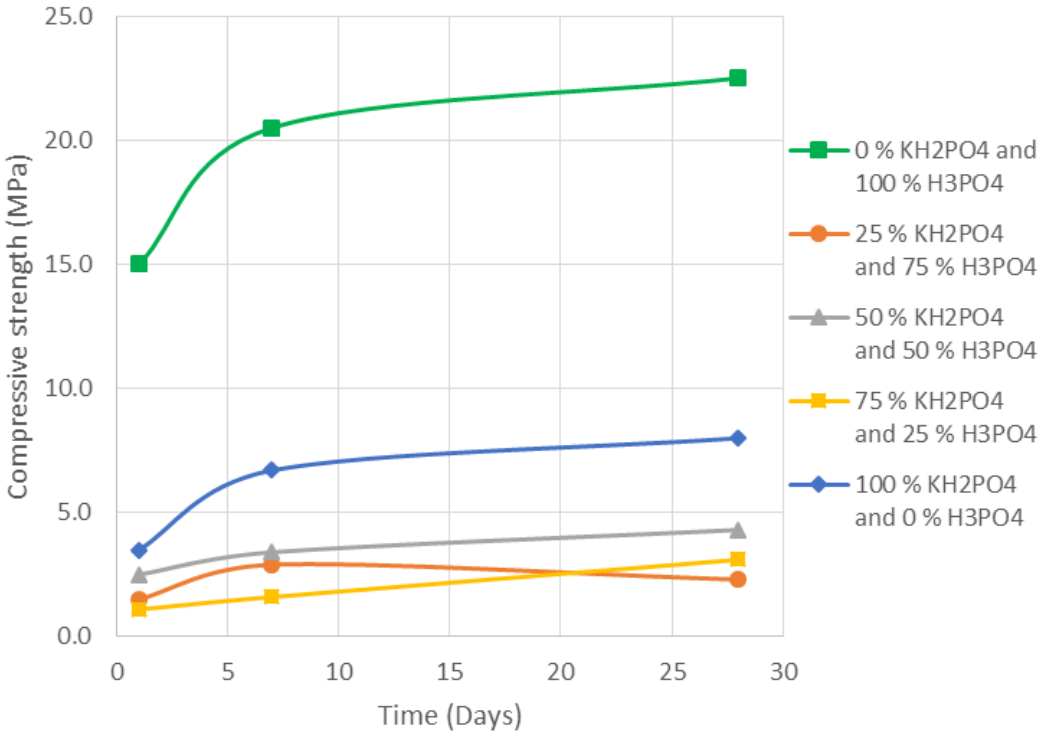

Figure 4.11 Comparison of compressive strengths of paste samples, prepared with combinations of H_3PO_4 and KH_2PO_4.

4.1.8 Acid vs. acid salt comparison

Figure 4.12 compares the strength of samples made with the 40, 50 and 60 wt% acid solutions and corresponding acid salts. As previously mentioned, paste samples prepared with 60 wt% acid solution can reach compressive strengths of 22 MPa, where the sample prepared with corresponding concentration of acid salt gain only 8 MPa strength. Lower concentrations, for both acid and acid salt, exhibit much lower strength. In addition the strength loss, is observed in only samples with 50 wt% or lower acid concentrations or with the solution-to-powder ratios lower than 1.0 whereas in the case of acid salts, enduring growth of strength, at all concentrations, is apparent.

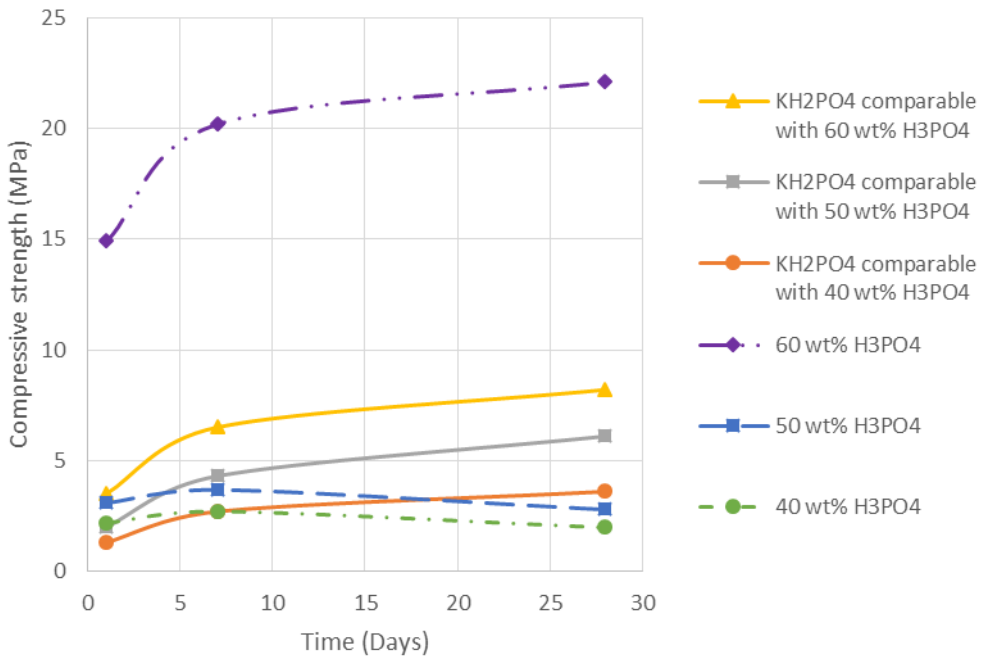

Figure 4.12 Compressive strength comparison between products made with H_3PO_4 and KH_2PO_4.

4.2 pH investigation

The pH values of the different mixtures were measured seeking a connection between the strength of produced CBPCs and the concentration, amount, and type of activation solutions. Figure 4.13 gives the acid solution neutralization by the AE fly ash. It can be seen that acid solution pH increases with time. The rate of this increase, which can be interpreted from the slope of the curves, subdivide the curves into two groups. The first group has relatively positive values of slope in contrast with the second group which shows a slower increase in pH. All of the 50 wt% acid solutions, which belong to the first group, were neutralized by the fly ash with a constant regime with time. In this group, increase in the amount of acid solution shows decrease in pH values of mixtures at the end of 24 h. This behavior can be seen up to the mixture with 60 wt% acid and solution-to-powder ratio equal to 1.0. After that, the second group with lower slope were observed. This alteration in curves slope shows that, beyond a specific concentration, the neutralization slows down and this causes an interruption in ceramic structure formation, based on compressive strength results. Actually the greatest compressive strengths belong to the mixture which has the slowest linear neutralization.

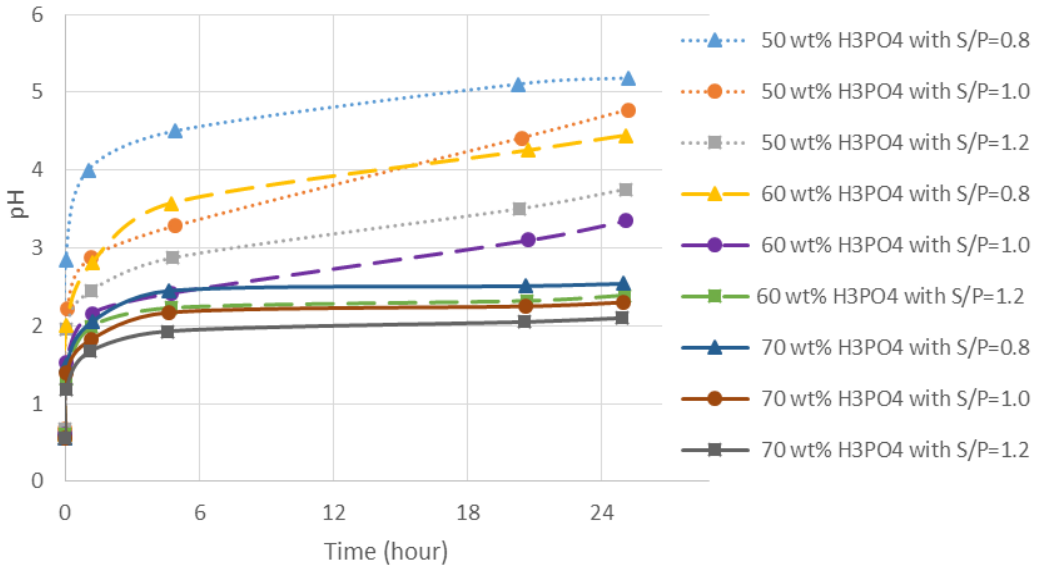

Figure 4.13 change in pH of the fly ash samples activated with H_3PO_4.

Figure 4.14 shows that KH_2PO_4 provides a pH higher than 5.5, immediately after mixing. For even the most concentrated mixture. By keeping constant the phosphate ions coming from both acid and acid salt, the poor performance of this acid salt in producing ceramics with AE fly ash can be related to the rather high pH it provides to the mixtures. The highest compressive strength belongs to 60 wt% phosphoric acid solution with solution-to-powder ratio of 1.0, which reached a pH of 3.3 after 24 h whilst the pH values of all acid salt mixtures are between 5.5 and 8 at the first 24 h of the reaction.

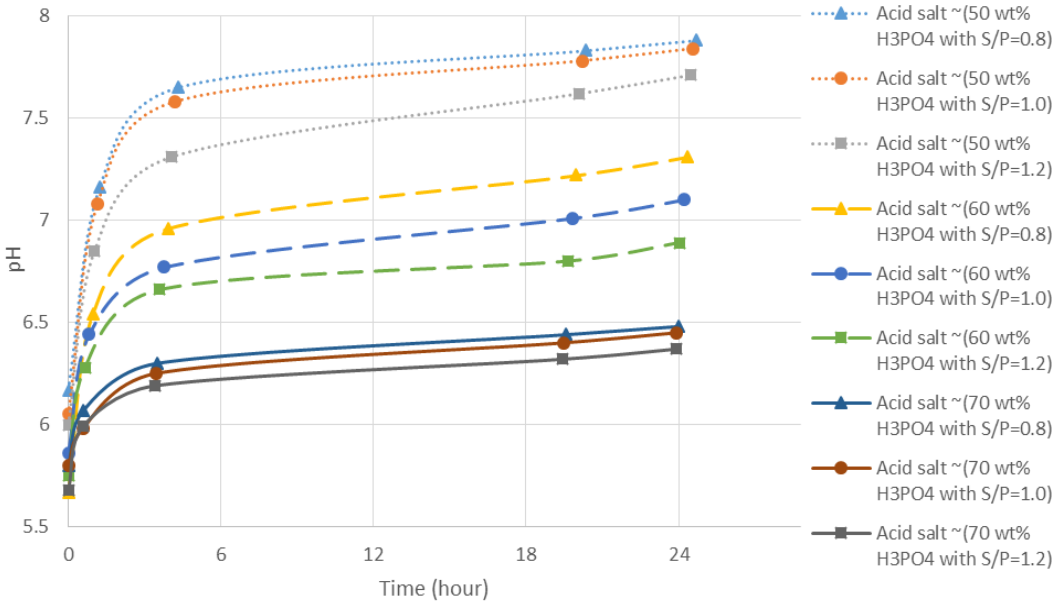

Figure 4.14 changes in pH of samples of the fly ash activated with KH_2PO_4.

4.3 Isothermal calorimetry

Figure 4.15 shows the normalized heat flow curves of the AE fly ash and various concentrations of acid/acid salt in the first 15 minutes of the reactions. The heat flow values were normalized by the mass of powder to yield units of w/g of powder. The reaction between fly ash and an acid or an acid salt is exothermic and this can be clearly seen in the graph. The heat produced by acid reactions was more than 4 times higher than the heat produced from acid salt reactions. The acids reactions, reached their peaks in approximately one minute. After that, for reactions with 40 and 50 wt% phosphoric acid, they tended to cool down quickly, however the 60 wt% acid reaction curve peaked for about 3 minutes with a slight increase in value and then tended to descend.

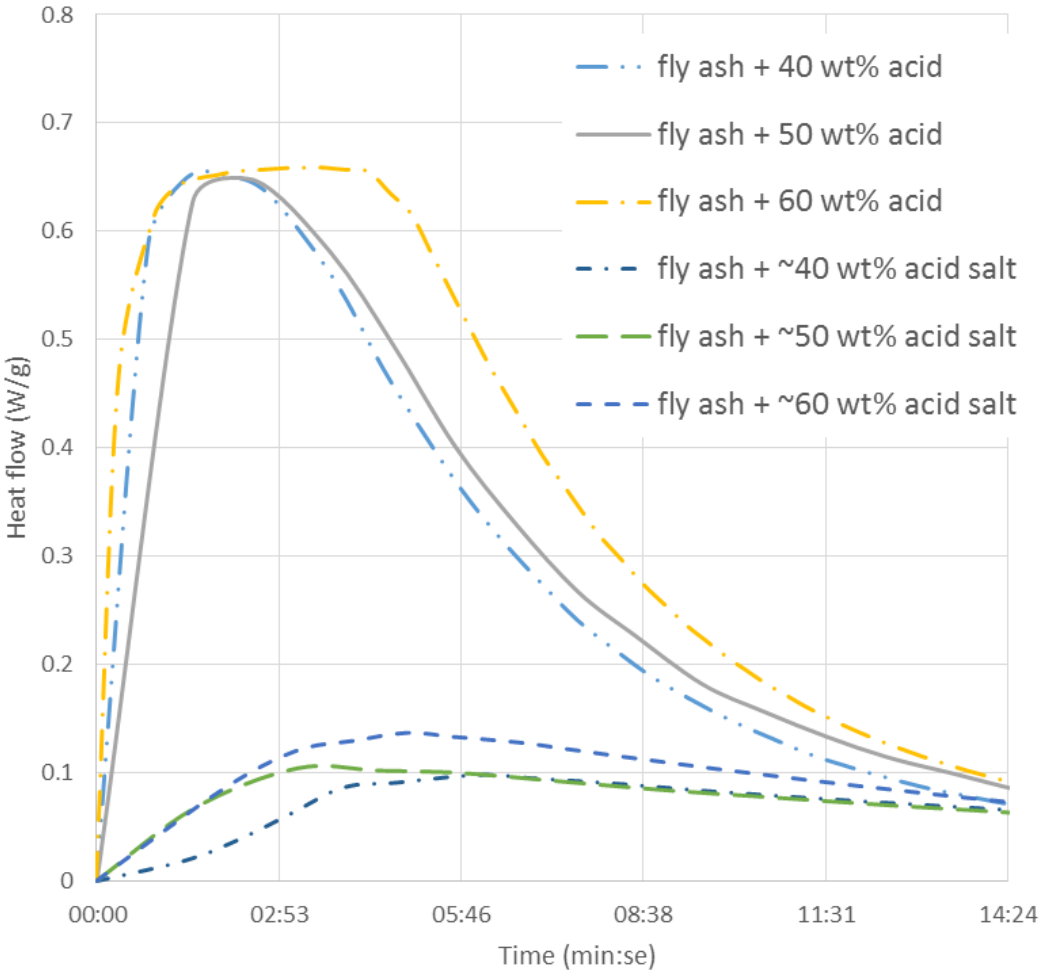

Figure 4.15 Normalized heat flow curves of the reactions of the AE fly ash and various concentrations of H_3PO_4 and KH_2PO_4 .

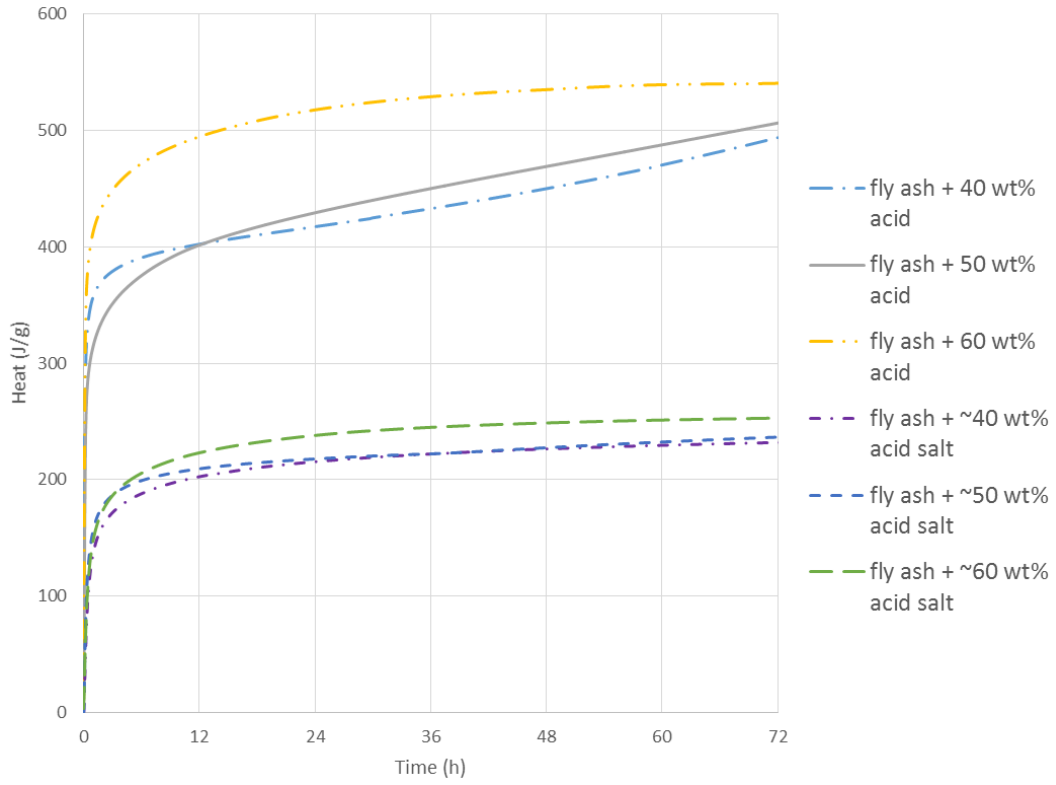

Figure 4.16 The curves of normalized cumulative heat of various concentrations of H_3PO_4 and KH_2PO_4 reactions with the AE fly ash.

Figure 4.16 gives the cumulative heat generated by the acid-base reactions over a 3-day period. It can be seen that the overall heat generation from AE fly ash and an acid solution reaction was approximately twice its reaction with the acid salt. The generated heat via 60 wt% phosphoric acid was much higher than the other acid concentrations.

4.4 SEM investigation

4.4.1 Fly ash and phosphoric acid paste

Four different structural patterns were observed in the SEM images of fly ash activated by 60 wt% phosphoric acid solution. Figure 4.17a exhibits three of these structures. First one is plain plate shapes at the top part of the image which has been magnified in Figure 4.17c. They are silicon rich crystals with aluminum and calcium phosphates. In the middle part, needle-shaped well-ordered calcium phosphate crystals were observed as the second pattern. Figure 4.17d shows these crystals. They are less than 2 μm in width with various lengths. The third pattern was a cloud-shaped pattern, observed in the lower part of Figure 4.17a, Figure 4.17i and Figure 4.17j. Their compositions were more compile than the first two. They contained of silicon, aluminum and calcium phosphates with carbon and sulfur inside. In addition, micro cracks were observed in the structure of this pattern. The lateral expansion of calcium sulfate or similar composition might be the reason of these micro cracks. Figure 4.17g and Figure 4.17h shows a bulk structure with compile composition again with higher amounts of silicon and aluminum with calcium and magnesium phosphate. There is no sign of sulfur in this structure while no micro cracks can be seen as well. The fourth pattern (Figure 4.17d and 4.17e) was related with a melted shape pattern with various-size hollow spheres inside. Table 4.9 shows the elemental composition of these patterns. In the absence of carbon and sulfur, silicon and aluminum were the main constituents of these patterns with some magnesium, iron, calcium, potassium and phosphate as well.

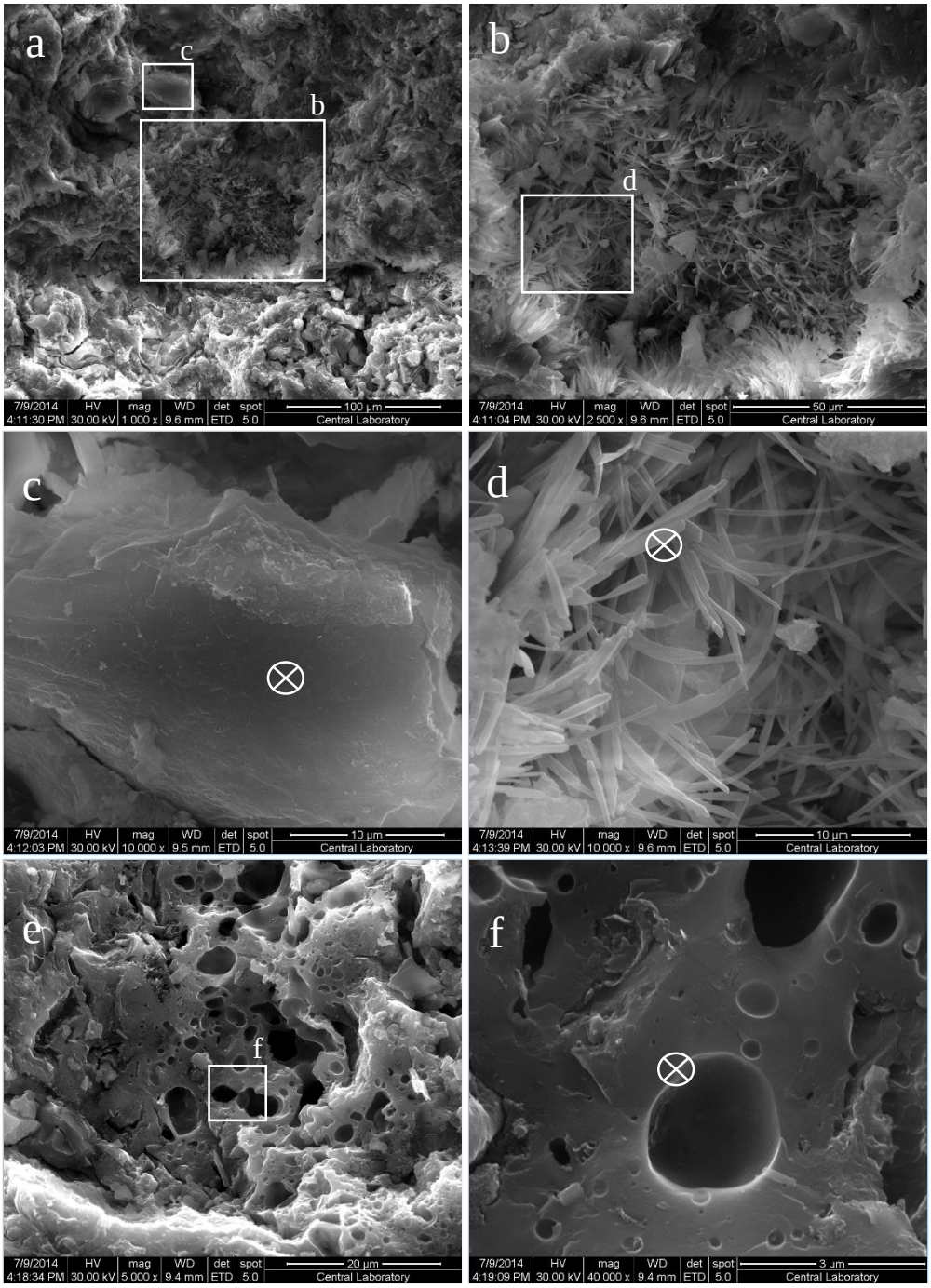

Figure 4.17 SEM images of the ceramic produced by AE fly ash and 60 wt% phosphoric.

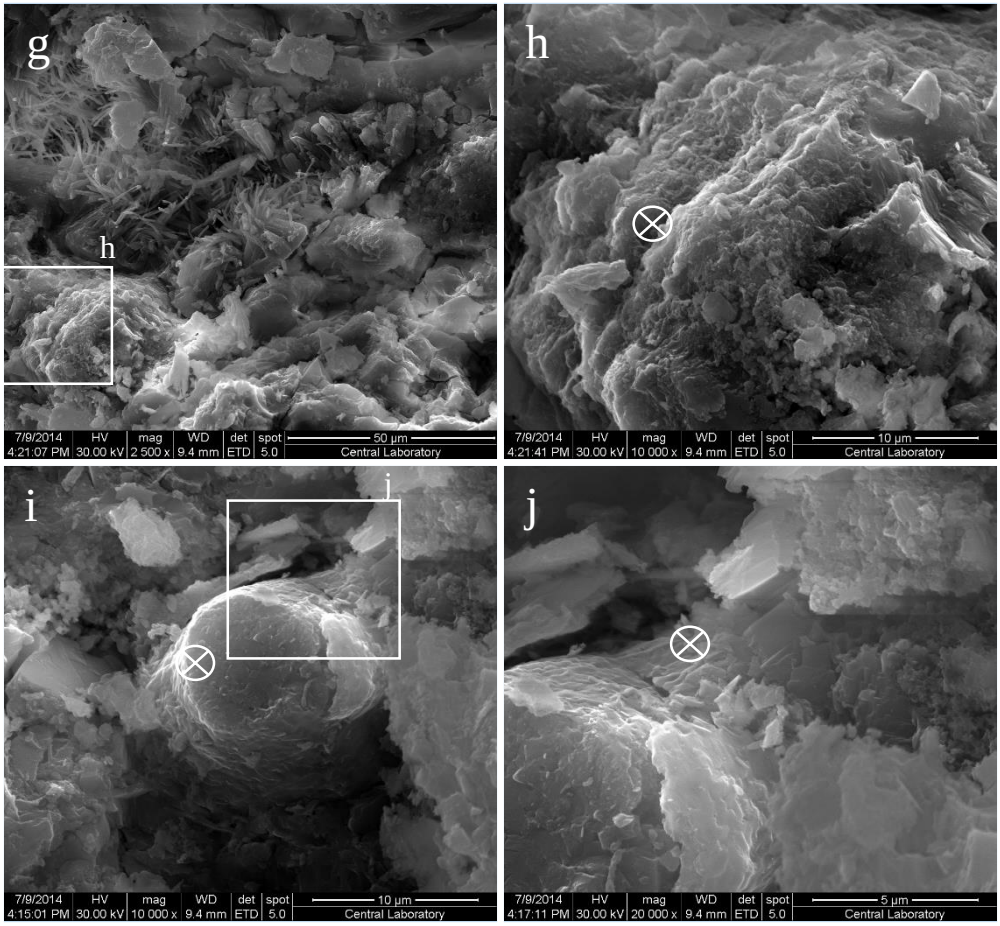

Figure 4.17 (continued).

Table 4.9 EDX quantitative analysis from various points of the AE fly ash and phosphoric acid paste.

Element	EDX analyzed points from Figure 4.17 (wt%)					
	c	d	F	h	i	j
O	44.60	37.26	44.39	44.45	38.00	40.39
Ca	4.42	29.74	2.68	1.91	13.53	19.20
P	7.90	19.67	1.74	3.36	18.05	16.30
C	0	13.39	0	14.20	15.90	13.64
Al	1.97	0	13.89	15.39	5.77	2.76
Si	41.12	0	30.16	19.87	3.94	2.51
Mg	0	0	1.58	0.29	1.32	0
K	0	0	1.91	0.53	0	0
Fe	0	0	3.67	0	1.83	1.85
S	0	0	0	0	1.66	3.43

4.4.2 AE fly ash and KH_2PO_4

Figure 4.18 shows the SEM images of paste made of AE fly ash and monopotassium dihydrogen phosphate as the acid salt. In these mixtures, mass of the acid salt was considered to have phosphate ions and water content equal to 60 wt% phosphoric acid solution at a solution-to-powder ratio of 1.0. Figure 4.18a shows a general view of a broken paste particle surface. Three noticeable points in this image are, the smooth and plane part at top, a hump shape similar to an unreacted fly ash particle on the left side and micro cracks in the middle. Although Figure 4.18e has similar crack in it. In addition, Figure 4.18f, exhibits a shell-shaped thin crystal structure.

Table 4.10 EDX analysis of the Figure 4.18.

Element	EDX analyzed points from Figure 4.18 (wt %)				
	b	c	d	e	f
O	31.73	36.94	37.79	31.14	51.19
Ca	21.03	7.72	15.90	18.72	4.10
P	2.55	14.61	11.16	11.16	3.64
C	0	12.35	0	10.61	9.17
Al	9.84	4.05	6.65	3.44	3.32
Si	25.14	7.42	15.22	7.96	17.63
Mg	1.62	0.88	1.05	0.88	0
K	4.06	14.24	9.53	11.68	9.39
Fe	4.01	1.88	2.70	3.83	0
Na	0	0	0	0	1.57
S	0	0	0	0.60	0

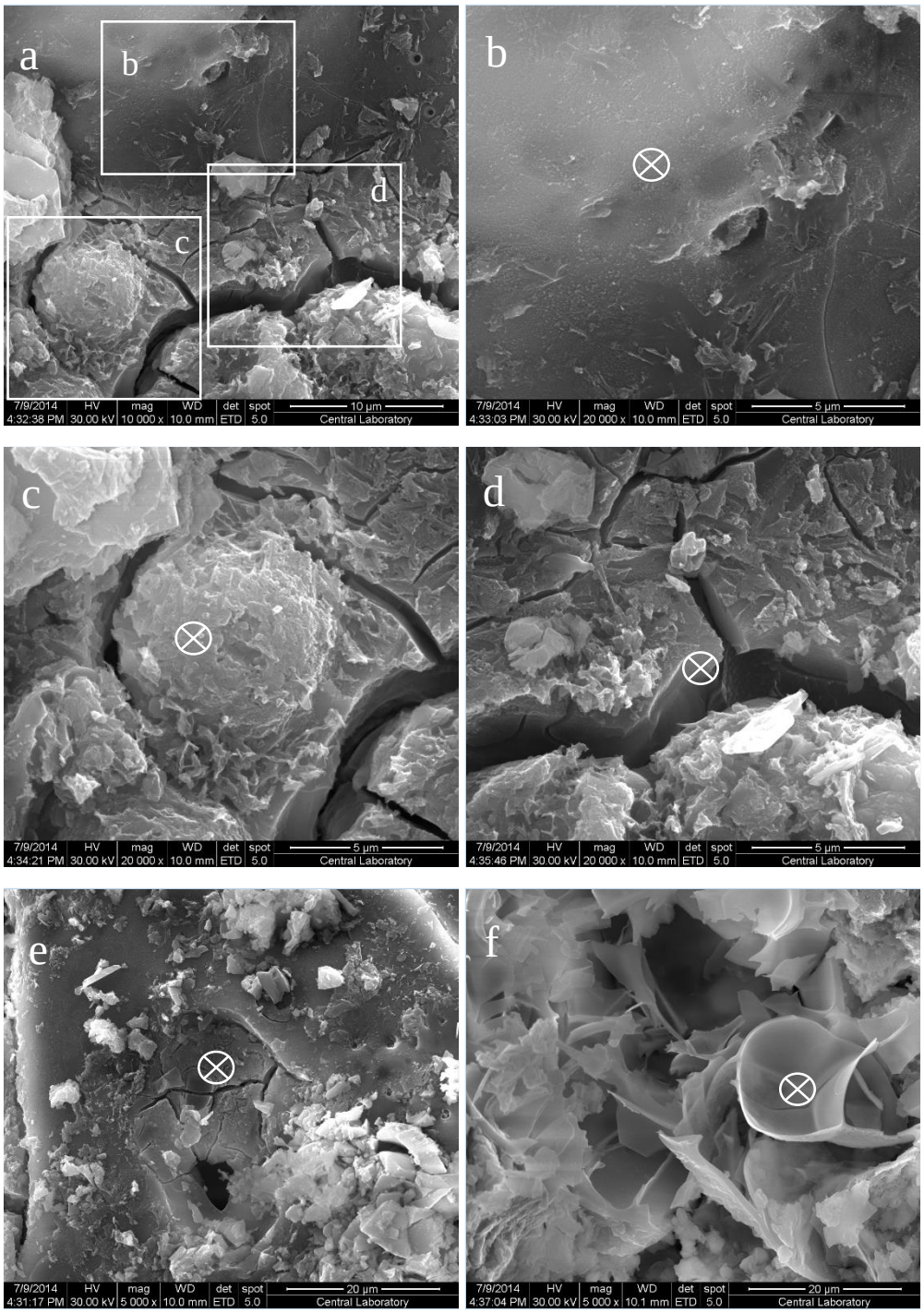

Figure 4.18 SEM images of the ceramic produced by AE fly ash and KH_2PO_4.

4.4.3 60 wt% phosphoric acid and AE fly ash paste with retarder

Figure 4.19 shows the general view of the CBPC made with the retarder. Although the retarder contained boron, which had the act of retardant in acid base reaction, but because of the equipment technical limitations, it was not observed in the EDX results. Distribution of needle-shaped crystals are more common than the samples without the retarder. Table 4.11 reveals the composition of these needle-shaped crystals is similar to the ones observed in Figure 4.17d. Figure 4.19e shows a gel form solidification with micro cracks in it. Table 4.11 gives the elemental composition of this pattern which mostly contains aluminum, silicon, and calcium phosphate.

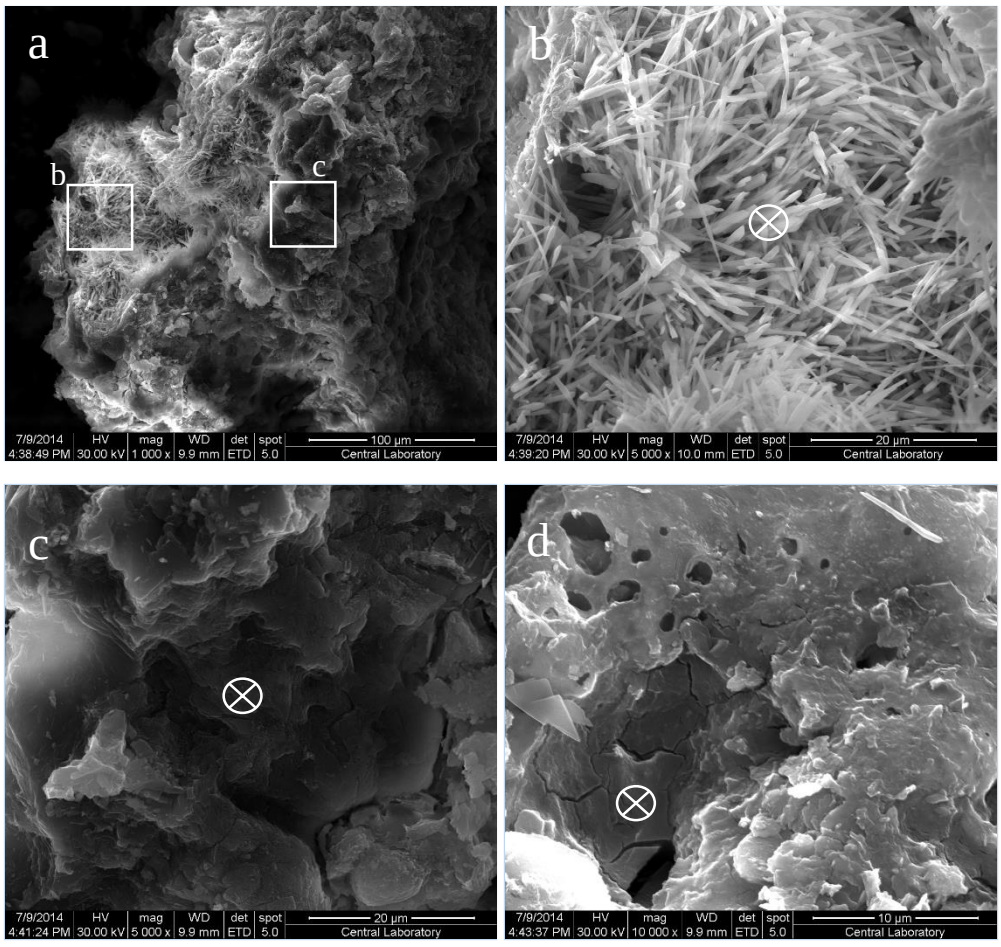

Figure 4.19 SEM images of the ceramic produced with AE fly ash and 60 wt% phosphoric acid solution and boron containing retarder.

Table 4.11 EDX quantitative analysis results of Figure 4.19.

Element	EDX analyzed points from Figure 4.19 (wt %)		
	b	c	d
O	42.44	37.73	41.17
Ca	25.14	16.07	5.76
P	11.11	18.82	3.68
C	20.90	12.62	0
Al	0	0	12.08
Si	0	0	30.32
Mg	0	0	1.78
K	0	0	1.45
Fe	0	0	3.77
S	0.42	0	0

4.4.4 AE fly ash and 60 wt% phosphoric acid solution paste, loaded by 10% glass

Figure 4.20 shows the morphology of fly ash and phosphoric acid paste loaded with 10 wt% of soda lime glass. Two dominant patterns in this case were: irregular-shaped structures seen in Figure 4.20a, Figure 4.20b, and Figure 4.20e and porous sponge-shaped structure at Figure 4.20c, which might occur due to a gel solidification. In addition, a small region consists of a titanium composition was seen. (Figure 4.20f). There were no signs of needle-shaped carbon and calcium phosphate crystals. Sulfur was detected in the sponge-shaped structure in which micro cracks were not observed. Few cracks were observed in body of the irregular-shaped structures, but not as much as in the samples of the previous figures.

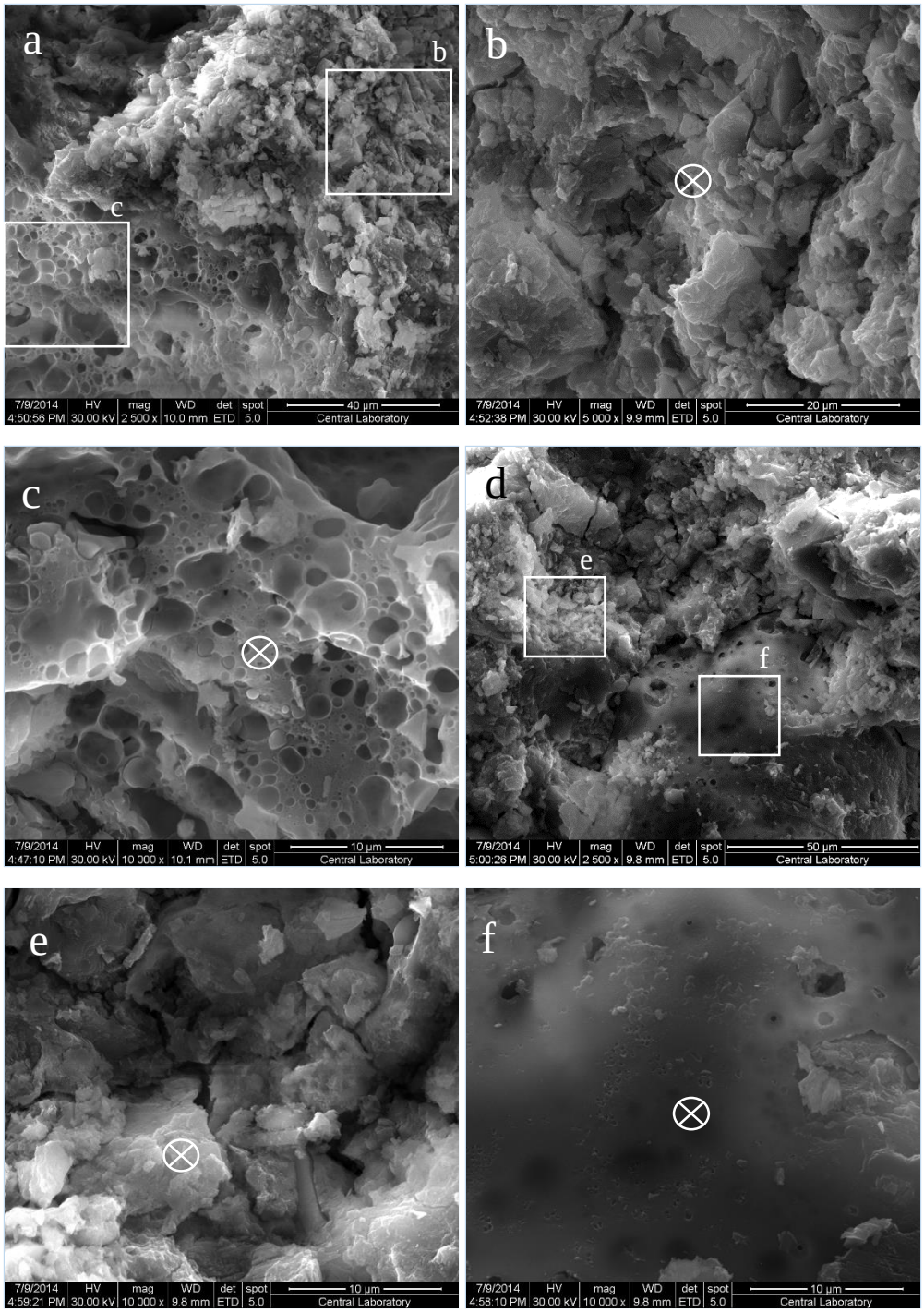

Figure 4.20 SEM images of AE fly ash and 60 wt% phosphoric acid solution paste loaded with 10% glass.

Table 4.12 EDX quantitative analysis results of the Figure 4.20.

Element	EDX analyzed points from Figure 4.20 (wt %)			
	b	c	e	f
O	25.15	28.21	40.16	37.95
Ca	23.31	29.16	22.64	5.51
P	7.14	14.35	21.26	1.34
C	25.68	16.48	0	0
Al	1.73	0	4.26	8.96
Si	2.56	1.50	7.59	17.3
Mg	0	0	0	1.41
K	0	0	0	0
Fe	14.44	2.94	4.08	6.19
S	0	7.36	0	0
Ti	0	0	0	21.34

4.4.5 40 wt% of AE fly ash, replaced with equal masses of glass and CAC, activated with 60 wt% phosphoric acid solution (S/P=1)

Figure 4.21 shows the heterogeneous pattern of the sample made with combination of the AE fly ash, soda lime glass powder and CAC, and phosphoric acid solution activated. Figure 4.21a is a complex phosphate composition with micro cracks within. Sulfur is seen among its constituents (Table 4.13). The pattern in Figure 4.21d, is similar to image Figure 4.21a. A gel type pattern with hollow bubbles inside, is in Figure 4.21c. Figure 4.21e and Figure 4.21f show a bunch of needle-shaped crystals with the same composition as those observed in previous samples. The cracks may have been formed due to be formed from expansion of a composition or shrinkage during solidification. The generated heat during acid base reaction may be capable in this case.

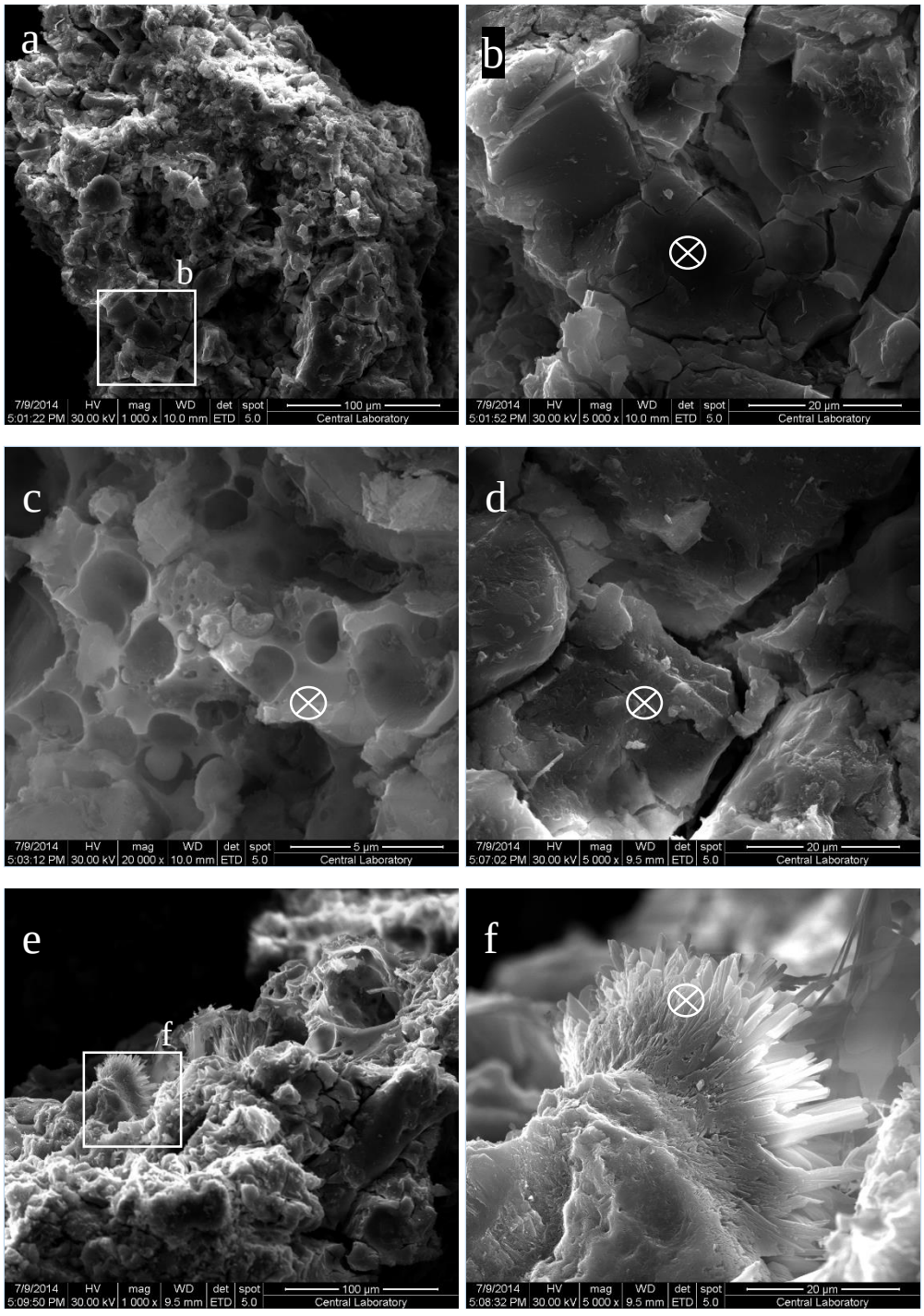

Figure 4.21 SEM images of AE fly ash, loaded with 20% glass and 20% CAC, activated with 60 wt% phosphoric acid.

Table 4.13 EDX quantitative analysis results of Figure 4.21.

Element	EDX analyzed points from Figure 4.21 (wt %)			
	b	c	d	f
O	46.83	23.16	51.31	45.51
Ca	10.87	22.24	8.64	18.33
P	16.22	9.80	12.89	16.15
C	11.13	0	10.95	19.29
Al	5.52	5.99	4.70	0
Na	1.00	0	1.14	0
Si	3.89	26.86	6.53	0.71
Mg	0.59	0	0	0
K	0	4.83	0.33	0
Fe	2.22	7.11	3.51	0
S	1.75	0	0	0

4.5 X-Ray Diffraction (XRD) Analysis

4.5.1 XRD of AE fly ash powder

Figure 4.22 shows the diffractogram of the as received fly ash powder. The fly ash XRD pattern shows anhydrite ($CaSO_4$), calcium oxide (CaO), Quartz (SiO_2), hematite (Fe_2O_3), calcite ($CaCO_3$) and gehlenite (Ca_2Al [$AlSiO_7$]).

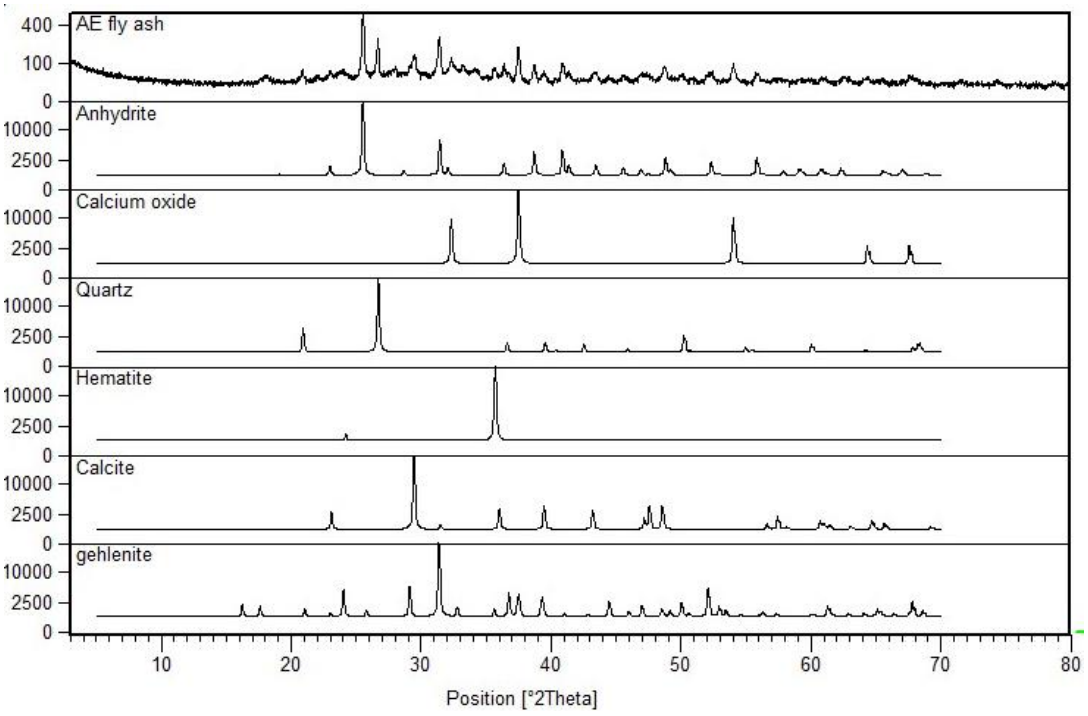

Figure 4.22 Diffractogram of AE fly ash powder.

4.5.2 XRD of the glass

Figure 4.23 exhibits the diffractogram of the glass powder. A big hump is seen in the XRD pattern at around 25 ˚2Ɵ which is an indication of the amorphous nature of the material. There are no distinctive peaks in this pattern to predict existing compounds.

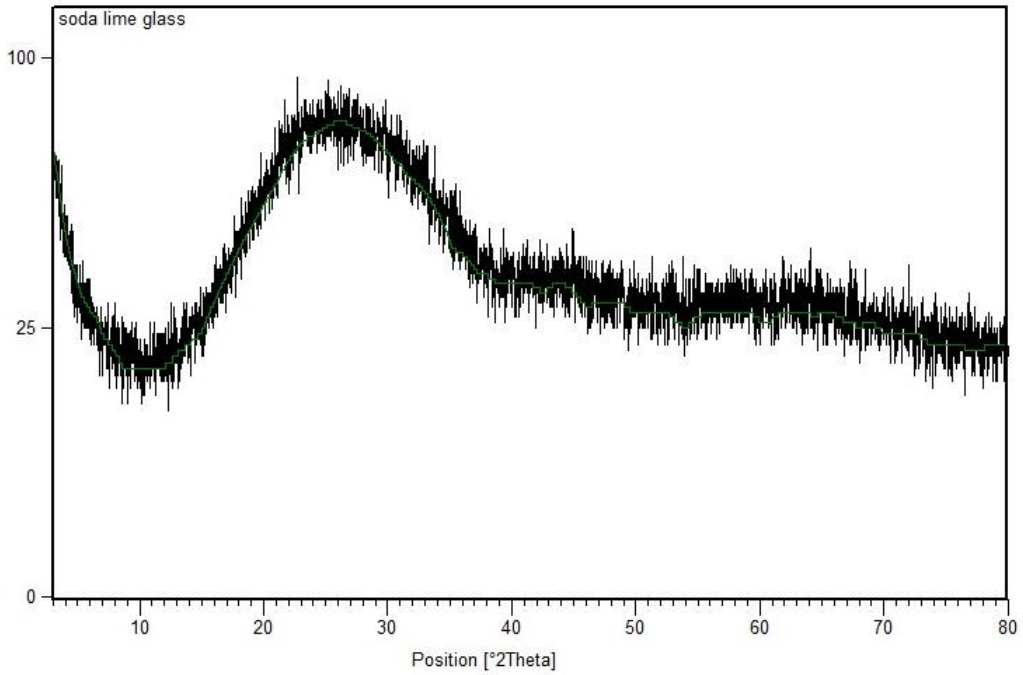

Figure 4.23 Diffractogram of the glass powder.

4.5.3 XRD of AE fly ash and H_3PO_4 product

The XRD peak assignment of paste made with AE fly ash and 60% phosphoric acid solution at S/P=1 is shown at Figure 4.24. This product is a composite material and has a multi-phase spectrum. The phases in this product are anhydrite ($CaSO_4$), quartz (SiO_2), brushite ($CaHPO_4 \cdot 2H_2O$) and monetite ($CaHPO_4$). The quartz and anhydrite are residuals of the unreacted AE fly ash so the dicalcium phosphate in the forms of brushite and monetite could be the main phases of this ceramic.

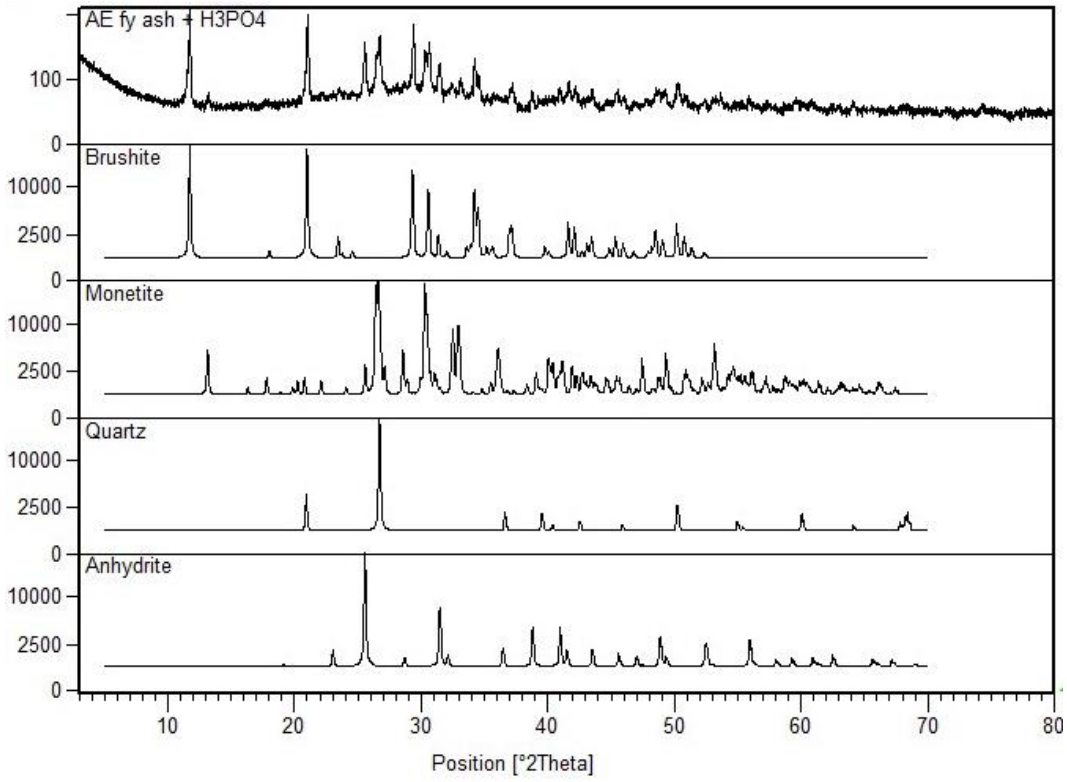

Figure 4.24 Diffractogram of AE fly ash activated by H_3PO_4.

4.5.4 XRD of AE fly ash and KH_2PO_4 product

Figure 4.25 shows the diffractogram of the paste made of AE fly ash and mono potassium dihydrogen phosphate and assigned phases. It is obvious from the main pattern that the product of AE fly ash and acid salt is significantly different than the product of the same powder activated with acid. Here the main phases are calcium magnesium phosphate ($CaMgP_2O_7$) and potassium calcium hydrogen phosphate ($K_3CaH(PO_4)_2$), and also quartz coming from the fly ash. Calcium sulfate was not seen in this pattern, whereas it was existing in previous products.

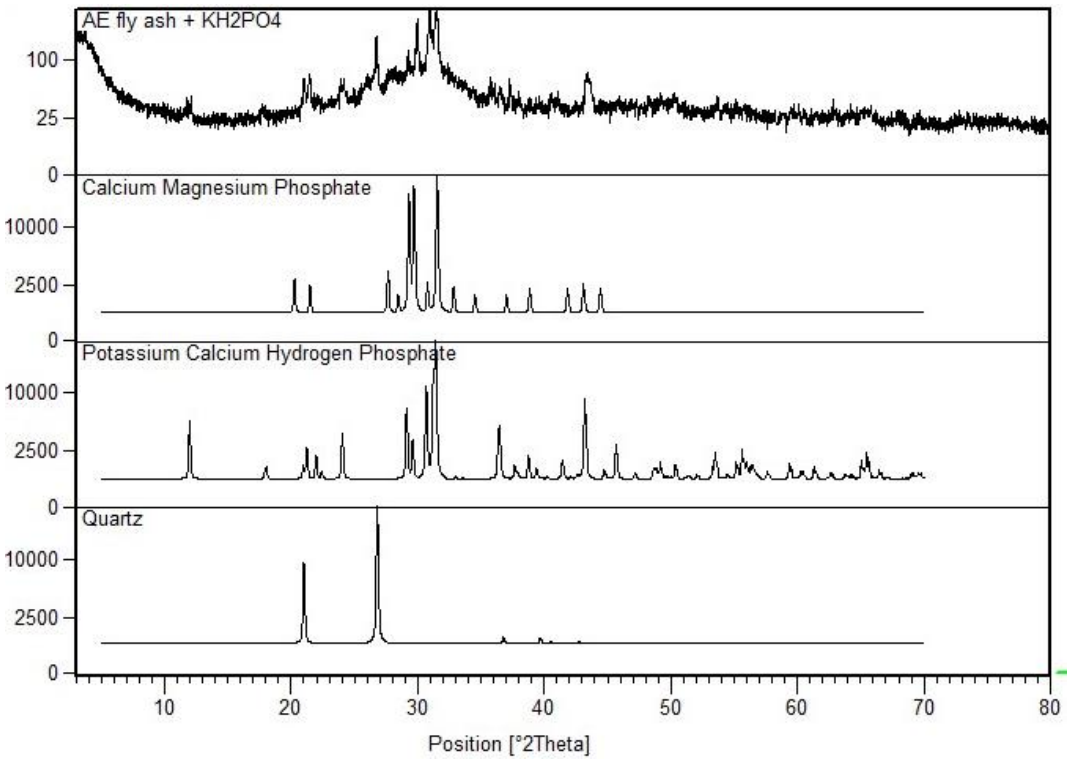

Figure 4.25 Diffractogram of AE fly ash activated by KH_2PO_4.

4.5.5 XRD of AE fly ash and H_3PO_4 product with retarder

Figure 4.26 gives the diffractogram of the fly ash activation with phosphoric acid at the presence of retarder (di-sodium tetraborate decahydrate). It is seen that the pattern is similar to the same product pattern obtained without the retarder. The main phase was brushite as Figure 4.24. An unknown peak was observed at 2Θ = 27.97 that didn't exist in either previous products or the raw materials.

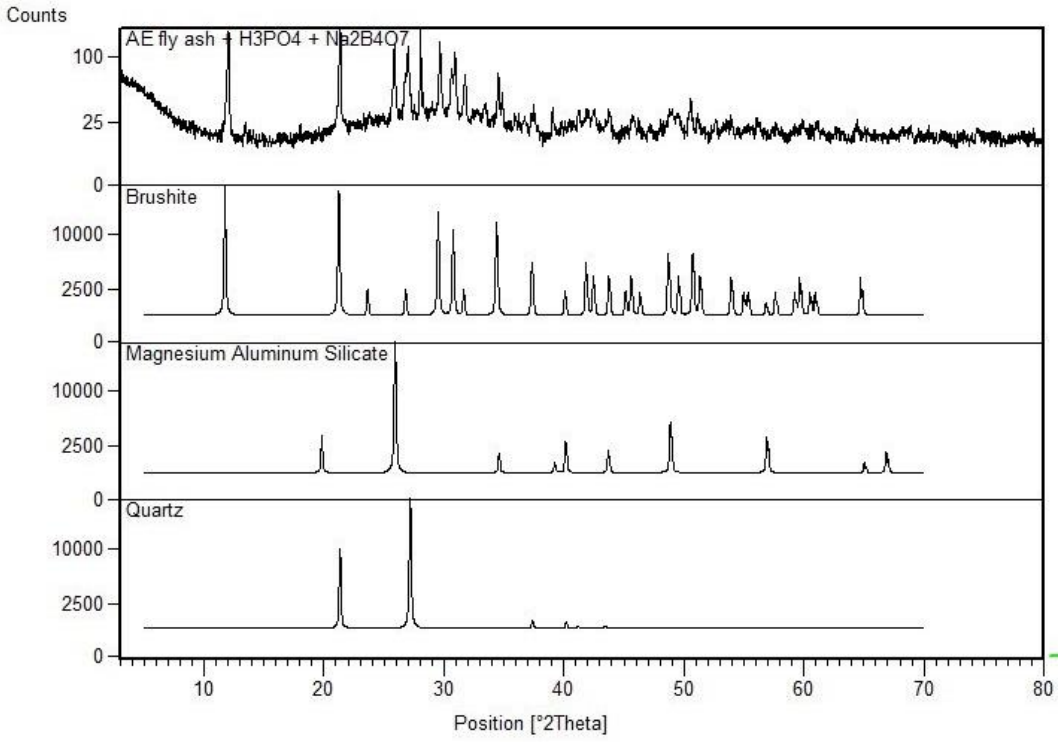

Figure 4.26 Diffractogram of AE fly ash activated by H_3PO_4 containing retarder.

4.5.6 XRD of AE fly ash loaded by 10 wt% glass and activated by 60 wt% phosphoric acid

Figure 4.27 gives the diffractogram of the ceramic produced by 10 wt% partially replacement of AE fly ash with soda lime glass and activated by phosphoric acid. The pattern is similar with the fly ash and phosphoric acid paste. Approximately all of the peaks have repeated, just their intensities are decreased. In addition a new peak was seen at 2Θ=23.83˚ which didn't exist in raw materials either. Calcium hydrogen phosphite ($CaH_4O_4P_2$) and sodium hydrogen phosphate ($H_2Na_5O_{11}P_3$) are two candidates with high probability of existing in this product structure. Calcium magnesium iron carbonate (ankerite) was another mineral which had a common peak pattern with analyzed product.

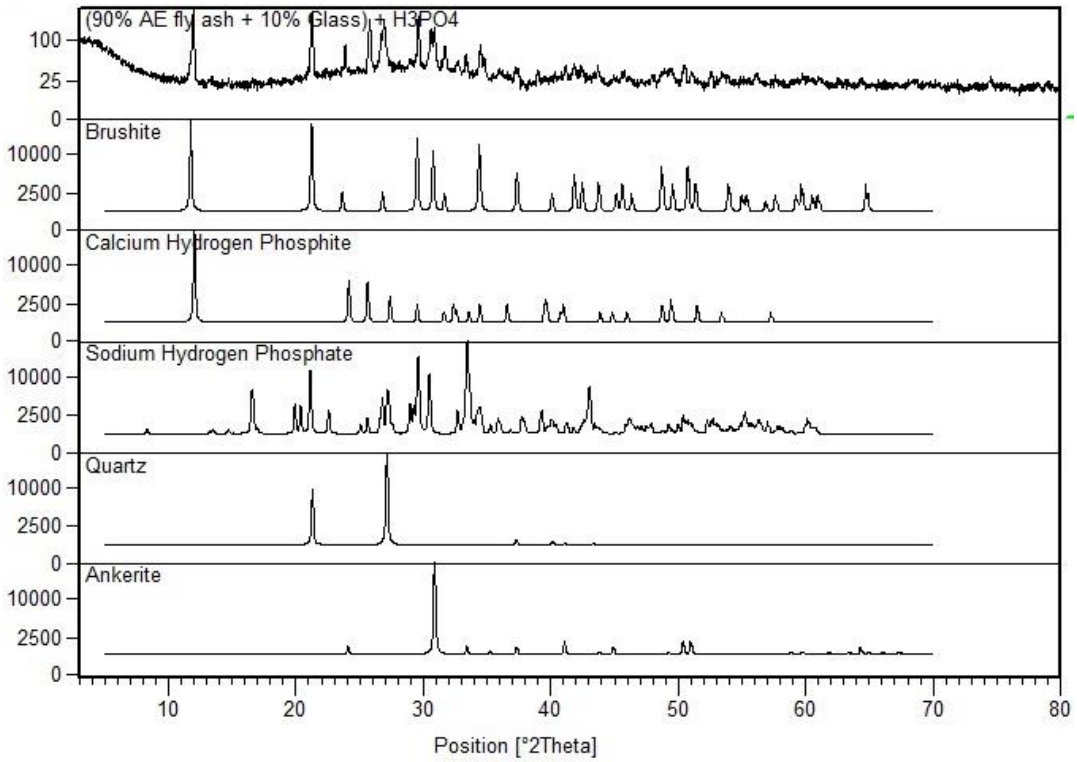

Figure 4.27 Diffractogram of AE fly ash and glass mixture activated with H_3PO_4.

4.5.7 XRD of 60 % AE fly ash, 20 % glass powder and 20 % CAC mixture activated with phosphoric acid solution

Figure 4.28 shows the diffractogram of product, prepared with a powder consisting of 60 wt% AE fly ash, 20 wt% soda lime glass, and 20 wt% CAC, activated by 60 wt% phosphoric acid solution with S/P=1. Brushite can be noted as the main phase of this ceramic. The same peaks with lower intensity were repeated in comparison with 100% fly ash produced ceramic with phosphoric acid in this analysis.

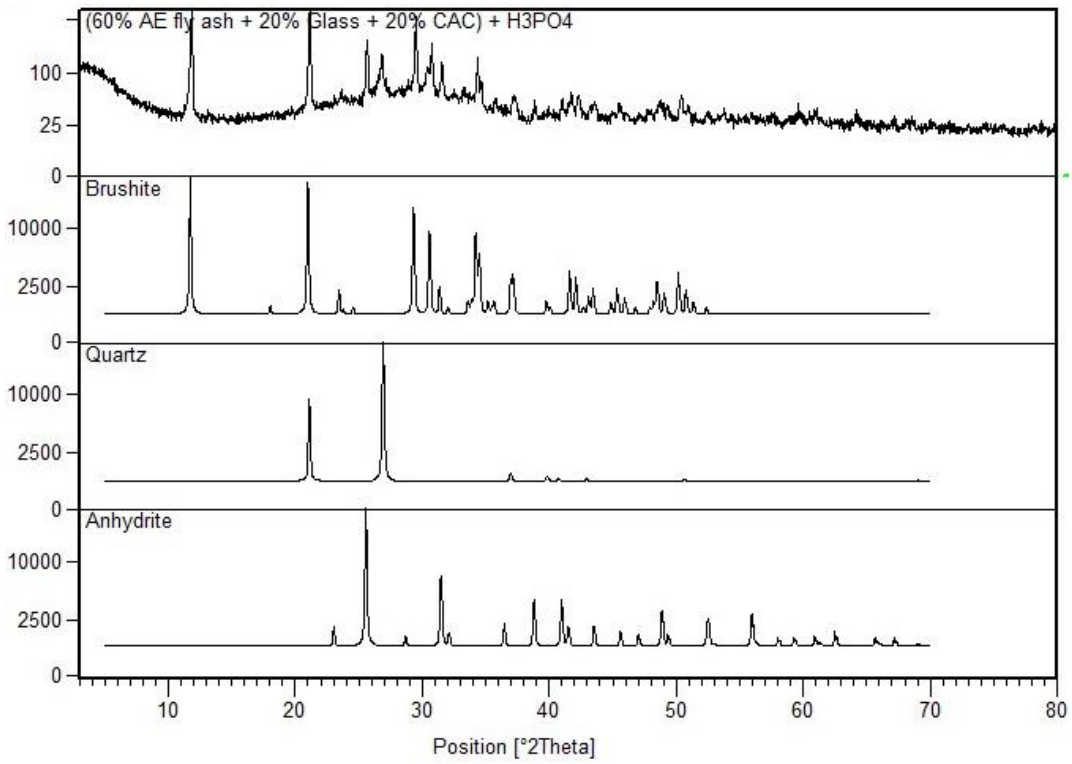

Figure 4.28 Diffractogram of the AE fly ash, glass and CAC mixture activated with H_3PO_4.

CHAPTER 5

CONCLUSIONS AND RECOMMENDATIONS

5.1 Concluding remarks

- In this study a waste material, which has almost no practical application in industry, was selected to be used as a constructional material. Afşin Elbistan fly ash was the waste candidate for investigating the possibility of fabricating phosphate-based ceramic. For this purpose, two activators were used: phosphoric acid and monopotassium dihydrogen phosphate. In addition, two different powders were utilized to change the main powder formulation: Calcium aluminate cement and soda lime glass.
- The chemical and mineral compositions of prepared samples and raw materials were investigated as well as their strength development and microstructures.
- Consolidation of powders was studied by activating with both acid and acid salt. Among the phosphoric acid solutions, 60 wt% acid solution produced the samples with the highest strengths. Phosphoric acid solution-to-powder ratio equal to one was seen to give the best performance for ceramic production. It was seen that phosphoric acid can produce ceramics with a higher compressive strength than the ones enhanced with monopotassium dihydrogen phosphate.
- The addition of 10 wt% soda lime glass to the mixture of AE fly ash and phosphoric acid, improved the 28-day product compressive strength by about 37 % over the 100 % fly ash control sample. This could be because of the chemical influence of glass compositions in overall acid-base reactions

and it could also be a physical effect of nucleation site seeding for crystal growth.

- SEM inspections revealed the crystal structure growth in products and XRD analysis identified these crystals: Brushite ($CaHPO_4 \cdot 2H_2O$) and Monetite ($CaHPO_4$) were the main crystal phase in the produced samples.
- A strength loss was noted between 7 and 28 days for most ceramics especially with acid solution concentrations lower than 60 wt% or solution-to-powder ratios lower than 1.0. Micro-cracks were also observed within the body of products. The further expansion of anhydrite or conversion of metastable phases within products could be the cause of this.

5.2 Recommendations for future work

- In this study the AE fly ash was investigated in as-received form. Different results can be obtained if ground, calcined, hydrated forms or chemical surface treatments methods would be investigated.
- The addition of soda lime glass powder to the mixtures, was a successful blending for a 28-day period, utilization of similar waste materials could improve the performance of produced samples.
- Long term inspections on produced samples would be useful for better understanding the durability issues of products.
- The influence of different retarding agents could be studied to enhance the workability of mixtures and achieving high performance products.

REFERENCES

Ahmaruzzaman, M. (2010). A review on the utilization of fly ash. *Progress in Energy and Combustion Science*, 36(3), 327-363.

ASTM C188. (2014). "Standard Test Method for Density of Hydraulic Cement," ASTM International, West Conshohocken, PA

ASTM C204. (2014). "Standard Test Methods for Fineness of Hydraulic Cement by Air-Permeability," ASTM International, West Conshohocken, PA

ASTM C595. (2012). "Standard Specification for Blended Hydraulic Cements," ASTM International, West Conshohocken, PA

ASTM C618. (2012). "Standard Specification for Coal Fly Ash and Raw or Calcined Natural Pozzolan for Use," ASTM International, West Conshohocken, PA

Christensen, J. H., & Reed, R. B. (1955). Density of Aqueous Solutions of Phosphoric Acid. *Industrial and Engineering Chemistry*, 47(6), 1277-1280.

Edvardsen, C., & Tollose, K. (2001). Environmentally "Green" Concrete Structures. In FIB Symposium: Concrete and Environment. Berlin.

Ferraiolo, G., Zilli, M., & Converti, A. (1990). Fly ash disposal and utilization. *Journal of Chemical Technology and Biotechnology*, 47(4), 281-305.

Ferreira, C., Ribeiro, A., & Ottosen, L. (2003). Possible applications for municipal solid waste fly ash. *Journal of Hazardous Materials*, 96(2-3), 201-16.

Fisher, G., & Prentice, B. (1978). Physical and morphological studies of size-classified coal fly ash. *Environmental Science & Technology*, 12(4), 447-451.

Gillberg, B., Fagerlund, G., Jönsson, Å., & Tillman, A.-M. (1999). *Betong och miljö: fakta från Betongforum. (Concrete and Environment: facts from Concrete)*

Iyer, R., & Scott, J., (2001). Power station fly ash - a review of value-added utilization outside of the construction industry. *Resources, Conservation and Recycling*, 31(3), 217-228.

Kingery, W. D. (1948). Phosphate bonding in refractories. (Doctoral dissertation).

Kingery, W. D. (1950). Fundamental Study of Phosphate Bonding in Refractories: I, Literature Review. *Journal of the American Ceramic Society*, 33(8), 239-241.

Kumar, R., Kumar, S., & Mehrotra, S. P. (2007). Towards sustainable solutions for fly ash through mechanical activation. *Resources, Conservation and Recycling*, 52, 157-179.

Laufenberg, T., Aro, M., & Wagh, A. (2004). Phosphate-bonded ceramic–wood composites: R&D project overview and invitation to participate. *Proceedings of Ninth International Conference on Inorganic-Bonded Composite Materials*, Vancouver, British Columbia, 1-12.

Mehta, P. K. (1999). Concrete Technology for Sustainable Development. *Concrete International*, 21(11), 47-52.

Mehta, P. K. (2004). High-performance, high-volume fly ash concrete for sustainable development. *In Proceedings of the International Workshop on Sustainable Development and Concrete Technology* (pp. 3-14).

Morgan, M. H., & Warren, H. L. (1960). Vitruvius: the ten books on architecture. New York: Dover.

Natarajan, R. (2005). Phosphate based oil well cements. (Doctoral dissertation).

Rossiter, B. W., Hamilton, J. F., & Baetzold, R. C. (1991). Physical Methods of Chemistry: Microscopy Vol.4, Wiley, New York City.

Roy, D. M. (1987). New strong cement materials: chemically bonded ceramics. Science, 235(4789), 651-658.

Roy, R., Agrawal, D., & Srikanth, V. (1991). Acoustic wave stimulation of low temperature ceramic reactions: The system Al_2O_3-P_2O_5-H_2O. *Journal of Materials Research*, 6(11), 2412-2416.

Roy, W., Thiery, R., Schuller, R., & Suloway, J. (1981). Coal fly ash: a review of the literature and proposed classification system with emphasis on environental impacts. Illinois State Geological Survey.

Sarkar, A. (1990). Phosphate cement-based fast-setting binders. *American Ceramic Society Bulletin*, 69(2), 234-238.

Türker, P., Erdoğan, B., Katnaş, F., & Yeğinobali, A. (2009). Türkiye'deki Uçucu Küllerin Sınıflandırılması Ve Özellikleri. Türkiye Çimento Müstahsilleri Birliği.

Ural, S. (2005). Comparison of fly ash properties from Afşin-Elbistan coal basin, Turkey. *Journal of Hazardous Materials,* 119(1-3), 85-92.

Wagh, A. (2004). Chemically bonded phosphate ceramics: twenty-first century materials with diverse applications. Elsevier Sci Ltd.

Wagh, A., & Jeong, S. (2002). Chemically bonded phosphate ceramics of trivalent oxides of iron and manganese. US Patent 6,498,119.

Wagh, A., & Jeong, S. (2003). Chemically bonded phosphate ceramics: I, A dissolution model of formation. *Journal of the American Ceramic Society*, 86(11), 1838-1844.

Wilson, A. D. (1978). The chemistry of dental cements. *Chem. Soc. Rev*., 7(2), 265-296.

Wilson, A. D., & Nicholson, J. W. (2005). Acid-base cements: their biomedical and industrial applications. Cambridge University Press. New York City

Wilson, A. D., Paddon, J. M., & Crisp, S. (1979). The hydration of dental cements. *Journal of Dental Research*, 58(3). 1065-1071.